Journal of Water Process Engineering 80 (2025) 109061

Contents lists available at ScienceDirect

Journal of Water Process Engineering

journal homepage: www.elsevier.com/locate/jwpe

Impact of chlorinated methylparaben derivatives on drinking water biofilm structure and antibiotic susceptibility

Ana Rita Pereira [a], Inês B. Gomes [a], Mourad Harir [b,c], Ana R.L. Ribeiro [d], Ana M. Gorito [d], Lúcia Santos [a], Manuel Simões [a,*]

[a] LEPABE, ALICE, Faculty of Engineering, University of Porto, Rua Dr. Roberto Frias, 4200-465, Porto, Portugal
[b] Research Unit Analytical BioGeoChemistry, Helmholtz Munich, 85764, Neuherberg, Germany
[c] Chair of Analytical Food Chemistry, Technical University of Munich, 85354, Freising, Germany
[d] LSRE-LCM, ALICE, Faculty of Engineering, University of Porto, Rua Dr. Roberto Frias, 4200-465, Porto, Portugal

ARTICLE INFO

Editor: Jing Zhang

Keywords:
Chlorination
Drinking water distribution systems
Dual-species biofilms
Methylparaben-chlorinated by-products
Parabens transformation products

ABSTRACT

Chlorination is a disinfection strategy widely used in drinking water distribution systems that can lead to the formation of harmful disinfection by-products. Parabens, a class of emerging contaminants, can react with chlorine and form parabens transformation products (PTP). This study investigates the formation and biological impact of PTP resulting from the chlorination of methylparaben (MP) with free chlorine. Both mono-chlorinated MP (3-Cl-MP) and di-chlorinated MP (3,5-diCl-MP) were produced and the characteristics of 7-days-old dual-species biofilms of *Acinetobacter calcoaceticus* and *Stenotrophomonas maltophilia* exposed to these PTP were assessed. Although 3,5-diCl-MP reduced bacterial culturability, 3-Cl-MP and 3,5-diCl-MP exposure increased the number of viable but non-culturable (VBNC) cells of *A. calcoaceticus* from dual-species biofilms by 3- and 5-fold, respectively. Exposure to 3-Cl-MP also increased VBNC cells in dual-species biofilms and the biofilm thickness by 10 μm. Extracellular polymeric substances showed a 2-fold increase in polysaccharide content upon exposure to both PTP. Interestingly, while MP exposure increased bacterial tolerance to chlorine, PTP exposure enhanced susceptibility. Biofilms exposed to PTP showed higher reductions in total and culturable cells, increased numbers of cells with damaged membranes, and improved chlorine efficacy in reducing the biofilm extracellular protein and thickness. Furthermore, 3,5-diCl-MP exposure increased *S. maltophilia* susceptibility to minocycline and trimethoprim-sulfamethoxazole. These findings demonstrate the complex effects of PTP on DW biofilms and highlight the need to evaluate conventional disinfection strategies to protect DW from the impact of parabens and their chlorinated by-products.

1. Introduction

The widespread use of personal care products (PCPs) containing parabens has led to their persistence in water sources, with reported concentrations reaching up to 100 μg/L in wastewater and surface waters [1,2]. Despite the implementation of advanced, multi-stage treatment processes in wastewater treatment plants (WWTP) and drinking water treatment plants (DWTP), the complete removal of parabens remains challenging. As a result, trace levels of parabens have been detected along drinking water distribution system(s) - DWDSs [3], with the highest concentration reported to date being 6 μg/L in Egypt [4]. Methylparaben (MP) is the most widely used paraben across a broad range of PCPs, which contributes to its higher persistence in water sources, compared to other parabens [1,2]. Although recognized as safe (GRAS), parabens are also considered endocrine disruptors, leading to human health complications such as perturbations of the central nervous system, carcinogenic effects, disruption of thyroid function, and dysregulation of the immune system [5]. Parabens also impact aquatic organisms, similar to their effects in human health, and can bioaccumulate, leading to biomagnification [6].

In DWDSs, aside from environmental contamination with pollutants, biofilms (from 10^3 to 10^8 cells/cm^2) are still unavoidable [7,8]. Microbial cells within biofilms are embedded in extracellular polymeric substances (EPS), which offer protection against disinfectants and increase nutrient availability, supporting the survival and persistence of bacterial communities in DWDSs [9]. The co-occurrence of biofilms and parabens

* Corresponding author.
E-mail address: mvs@fe.up.pt (M. Simões).

https://doi.org/10.1016/j.jwpe.2025.109061
Received 5 August 2025; Received in revised form 9 October 2025; Accepted 2 November 2025
Available online 18 November 2025
2214-7144/© 2025 The Authors. Published by Elsevier Ltd. This is an open access article under the CC BY-NC-ND license (http://creativecommons.org/licenses/by-nc-nd/4.0/).

in these systems can also change DW biofilm ecology. Previous studies found that, even at trace levels (0.15 to 15 μg/L), parabens can alter bacterial behavior by increasing biofilm proliferation [10], enhancing antibiotic tolerance [11], and compromising water disinfection with increased bacterial resistance to chlorination [12]. These effects will inevitably affect DW quality and safety, having the potential to compromise the health of DW consumers.

Another major concern for DW safety is the formation of disinfection by-products (DBPs) occurring during water disinfection [13]. Besides water chlorination, chlorine can readily react with dissolved nutrients in bulk water and EPS components from biofilms, forming DBPs [7]. This potential to react also applies to other organic compounds in DWDSs, such as parabens. Due to the presence of hydroxyl groups in the aromatic ring, parabens are highly reactive with chlorine, undergoing electrophilic aromatic substitution reactions that lead to the formation of parabens transformation products (PTP), especially chlorinated parabens [14]. Although PTP are less studied than conventional DBPs, their occurrence has been documented in real WWTP [15], surface water [16], DW [17], and swimming pools [18], with reported concentrations reaching up to 293 μg/L, 13.4 μg/L, 0.3 μg/L, and 1.1 μg/L, respectively. So far, only two studies have reported the occurrence of PTP in DW, detecting di-chlorinated methylparaben (3,5-diCl-MP) and di-chlorinated ethylparaben (3,5-diCl-EP) at 0.17 and 0.07 ng/L, respectively, in Texas [19], and halogenated parabens at concentrations of up to several tens of ng/L in France [17]. The toxicological and ecological implications of PTP, including endocrine-disruptive effects and increased bioaccumulation potential, are emerging concerns. However, controversial conclusions remain when comparing their effects to those of original parabens [20]. Although there are no studies evaluating the effects of PTP on DW microbial dynamics, the formation of these compounds will compromise the efficacy of water disinfection by reducing the availability of free chlorine for microbial inactivation [21]. In addition, the formation of DBPs is also associated with increased bacterial resistance in water sources, which may lead to public health issues [22]. Therefore, a deeper understanding of biofilm dynamics within DWDSs in the presence of PTP is crucial for ensuring DW quality and safeguarding public health.

This study aims to fill this gap by studying the effects of methylparaben (MP) and MP-chlorinated by-products (3-Cl-MP and 3,5-diCl-MP) at 15 μg/L on bacterial physiological characteristics and tolerance to chlorine disinfection and antibiotics by a 7-day-old dual-species biofilm formed by *Acinetobacter calcoaceticus* and *Stenotrophomonas maltophilia*. The results provide a basis to help the development of monitoring and maintenance strategies to protect DW quality and safety by providing information about the effects of PTP on DW bacteria in water supply networks when such compounds are present.

2. Materials and methods

2.1. Parabens and chlorinated by-products selection

MP, procured from Sigma-Aldrich (Germany), was selected as a representative paraben since it is the most widely used in PCP and is commonly detected in water bodies [23]. The MP-derived PTP: monochlorinated methylparaben - 3-Cl-MP (TCI, Belgium) and dichlorinated methylparaben - 3,5-diCl-MP (GmbH, Germany) were selected based on their frequent identification as MP-chlorinated by-products after chlorination in water bodies and commercial availability [24]. The formation of these MP-chlorinated by-products upon MP reaction with free chlorine at 5 mg/L for 30 min was evaluated through analytical procedures (Section 2.2). The original paraben (MP) and both MP-chlorinated by-products were tested at 15 μg/L to replicate relevant concentrations encountered in water sources [10–12]. Parabens are found in water sources, such as WWTP effluents and surface waters, where concentrations can range from 10 ng/L [19] to 500 μg/L [25,26]. The selected concentration (15 μg/L) also mirrors the highest level of paraben contamination observed in DW - 6 μg/L [4]. Under extreme conditions, the full original paraben fraction (MP) could be converted to these by-products (3-Cl-MP and 3,5-diCl-MP). Therefore, by testing the selected transformation products at 15 μg/L, the designed experiments simulate an upper-bound scenario and allow direct comparison with the parent compound.

All stock solutions were prepared in sterile ultrapure water (UPW). The physicochemical properties and structures of MP and MP chlorinated by-products (3-Cl-MP and 3,5-diCl-MP), as well as the maximum concentrations reported in real water sources, are presented in Table 1.

2.2. Evaluation of the formation of MP-chlorinated by-products

The formation and identification of MP-chlorinated by-products were assessed using solid-phase extraction (SPE) followed by Fourier transform ion cyclotron resonance mass spectrometry (FT-ICR MS) analysis. For that, water samples (500 mL), including UPW and synthetic tap water (STW), both with and without MP addition at 15 μg/L, were reacted with free chlorine at 5 mg/L for 30 min. The concentration and contact time with free chlorine were chosen in accordance with the disinfection treatment used and described in Section 2.5.

2.2.1. Solid phase extraction

After 30 min of reaction, water samples were extracted using Bond Elut PPL cartridges (modified styrene-divinylbenzene polymer, 1 g sorbent in 6 mL cartridges, Agilent Technologies). The pH of the water samples was first adjusted to 2.5 using formic acid (≥99 %, HiPerSolv Chromanorm®) prior to extraction to enhance the retention of organic compounds. The cartridges were conditioned with methanol (10 mL, LC-MS Lichrosolv®), followed by acidified UPW (10 mL, pH 2.5, spectrophotometric grade), ensuring the packing material remained wet. After sample loading, the cartridges were washed with 10 mL of 0.1 % formic acid in water to remove residual ions of chlorine anion that could interfere with FT-ICR MS analysis. The cartridges were then dried under vacuum for 2 h and eluted with methanol (10 mL, LC-MS Lichrosolv ®). The extracts were collected in amber glass vials (40 mL) and stored at −20 °C until FT-ICR MS analysis. No quenching agent was used to avoid interference or misinterpretation during FT-ICR MS analysis.

2.2.2. Fourier transform ion cyclotron resonance mass spectrometry (FT-ICR MS) analysis

A Bruker Solarix 12 Tesla FT-ICR MS (Bruker Daltonics, Germany), equipped with a negative mode electrospray ionisation [ESI(−)] source, was used to identify chlorinated MP compounds. The instrument was operated with a spray current of −3.6 kV and a flow rate of 2 μL/min, and it was pre-calibrated using known arginine clusters. Blank samples were analysed between runs to prevent cross-contamination. Each spectrum was obtained by averaging 300 scans over a mass range of m/z 129–1000. Spectra were internally calibrated using an appropriate reference mass list, ensuring a mass accuracy of <0.2 mg/L error. Molecular formulas were assigned to m/z ions using in-house software developed at Helmholtz Munich (Germany), with the search limited to the following chemical elements: $^{12}C_{0-100}$, $^{16}O_{0-80}$, $^{1}H_{0-\infty}$, and $^{35}Cl_{0-5}$.

2.3. Bacteria and culture conditions

Acinetobacter calcoaceticus and *Stenotrophomonas maltophilia*, both Gram-negative opportunistic bacteria, were previously isolated from a DWDS by Simões et al. [27]. These bacteria, known to form biofilms, are common in DWDSs and are of potential public health concern, particularly because of their resistance to antibiotics and potential to infect immunocompromised individuals [28,29]. *A. calcoaceticus* has also the ability to coaggregate, playing a bridging function in biofilm formation and allowing the establishment of antimicrobial resilient biofilms [30].

Both bacteria were grown in R2A broth medium prepared as described by Gomes et al. [31], overnight at 25 °C with shaking (160

Table 1
Physicochemical properties and structures of MP and MP-derived chlorinated by-products.

Compound	CAS number	Molecular weight	Structure	log K_{OW}	pKa	Maximum concentrations
Methylparaben (MP)	99–76-3	152.15	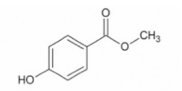	1.96	8.17	- WWTP: 560 μg/L [26]; - Surface water: 100 μg/L [25]; - DW: 6 ng/L [4]
Mono-chlorinated methylparaben (3-Cl-MP)	3964-57-6	186.6	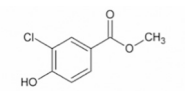	2.50	7.51	- WWTP: 61 ng/L [85]; - Surface water: 267 ng/L [16]; - DW: 1.9 ng/L [17]
Di-chlorinated methylparaben (3,5-diCl-MP)	3337-59-5	221.04	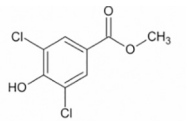	3.10	6.09	- WWTP: 152 ng/L [16]; - Surface water: 13.4 μg/L [16]; - DW: 7.9 ng/L [17]

Notes: log K_{OW} values were calculated based on chemical structures of compounds by https://www.molinspiration.com/cgi/properties and pKa through https://playground.calculators.cxn.io/. 3-Cl-MP is also known as methyl 3-chloro-4-hydroxybenzoate and 3,5-diCl-MP as methyl 3,5-dichloro-4-hydroxybenzoate.

rpm) in an orbital incubator (New Brunswick Scientific, I26, USA). After incubation, bacterial cells were harvested by centrifugation (Eppendorf centrifuge 5810R) at 3772 ×*g* for 10 min. Then, bacterial cells were resuspended in R2A broth adjusted to 2×10^7 colony-forming units - CFU/mL, for subsequent experimental procedures, to mimic the bacterial concentrations typically found in DWDSs [7].

2.4. Dual-species biofilm formation and exposure to MP-chlorinated by-products

Dual-species biofilms of *A. calcoaceticus* and *S. maltophilia* were grown on polypropylene (PPL) coupons (1 × 1 cm) in the presence and absence of 15 μg/L of MP, 3-Cl-MP, and 3,5-diCl-MP for 7 days as described by Pereira and Gomes [12]. After adjustment in R2A broth and incubation for 24 h, biofilms were washed with STW and subsequently exposed to R2A medium with and without MP, 3-Cl-MP, or 3,5-diCl-MP at 15 μg/L for an additional 24 h. After this period, biofilms were rewashed and exposed to STW supplemented with MP and their transformation products to mimic the low availability of nutrients in real DWDSs. This procedure was repeated every two days for up to 7 days of growth. STW was composed by 100 mg/L $NaHCO_3$ (Fisher Scientific, UK), 13 mg/L $MgSO_4.7H_2O$ (Merck, Germany), 0.7 mg/L K_2HPO_4 (Aplichem Panreac, Germany), 0.3 mg/L KH_2PO_4 (Chem-Lab, Belgium), 0.01 mg/L $(NH_4)_2SO_4$ (Labkem, Spain), 0.01 mg/L NaCl (VWR, Belgium), 0.001 mg/L $FeSO_4.7H_2O$ (VWR PROLABO, Belgium), 1 mg/L $NaNO_3$ (Labkem, Spain), 27 mg/L $CaSO_4$ (Labkem, Spain), 1 mg/L humic acids (Sigma-Aldrich, Germany). The growth period of biofilms (7 days) was sufficient to simulate biofilms with a mature state in cell density, mass and metabolism, resembling these sessile structures encountered in DWDSs [32].

Coupons of PPL were selected as representative pipe materials from DW networks, where pronounced modifications on biofilm characteristics were observed with the exposure to parabens [10,12,33]. These polymeric materials were previously cleaned and sterilised before being placed horizontally inside each well of 24-well microtiter plates for biofilm formation following the procedure detailed in Gomes et al. [31]. Dual-species biofilms were formed by adding 0.5 mL of each bacterial suspension adjusted to 2×10^7 CFU/mL in each well.

2.5. MP-chlorinated by-products exposure on dual-species biofilm tolerance to disinfection

After 7 days of growth, dual-species biofilms exposed and non-exposed to MP, 3-Cl-MP, and 3,5-diCl-MP were treated with sodium hypochlorite - NaOCl (Acros Organics, USA) at 5 mg/L of free chlorine for 30 min, following the procedure described by Pereira and Gomes [12]. This sequential exposure design (initial exposure to MP and their transformation products followed by chlorine treatment) was selected to assess how continuous exposure influences biofilm development and characteristics, and to evaluate whether these changes alter bacterial tolerance to disinfection. The free chlorine concentration (5 mg/L) selected represents the maximum allowed in DW according to WHO guidelines, which also recommends a contact time of 30 min with free chlorine to ensure microbiological safety of water before entering distribution systems [34]. Briefly, the bacterial suspension was removed, and each coupon was rinsed with 1 mL of sterile STW to remove weakly adhered or planktonic cells. Free chlorine concentration (5 mg/L) was previously adjusted through N, N-diethyl *p*-phenylenediamine (DPD) method [35]. A volume of 1 mL of sodium thiosulfate (0.5 % w/v) (Labkem, Spain) was added to each well for 10 min to neutralise chlorine activity after chlorine treatment [36]. The same procedure was performed for non-treated dual-species biofilms by substituting free chlorine solution with STW. Biofilms non-exposed and exposed to MP and MP-chlorinated by-products (3-Cl-MP and 3,5-diCl-MP), and biofilms treated and non-treated with free chlorine, were then characterised in terms of cell culturability, density, membrane integrity, and VBNC cells. The biofilm structure and thickness analysis was assessed using optical coherence tomography (OCT). The EPS quantification in terms of proteins and polysaccharide concentration was also performed. In addition, the spatial organisation of EPS components on dual-species biofilms exposed and non-exposed to MP and MP-chlorinated by-products was evaluated through Confocal Laser Scanning Microscopy (CLSM).

2.5.1. Biofilm culturability, density, membrane integrity, and viable but non-culturable cells

Coupons containing biofilms were inserted in a 15 mL centrifuge tube containing 5 mL of sterile saline (0.85 % w/v) and vigorously vortexed for 2 min (to ensure the complete removal of adhered bacteria and the dissociation of possible bacterial aggregates without compromising bacterial viability). This biofilm suspension was used for further CFU, cellular density, membrane integrity, and VBNC cells quantification. The number of CFU/cm^2 was determined through the drop plate method, where bacterial cells (after appropriate dilutions in sterile saline - 0.85 % w/v NaCl) were plated in R2A agar (Merck, Germany) and incubated at 25 °C for 24 h, for cell counts. The detection limit (DL) for CFU enumeration was 2 log CFU/cm^2. Each bacterial strain in dual-species biofilms was differentiated from the others by morphological analysis of the colonies [10].

The number of total bacterial cells and bacteria with a damaged membrane was determined using the Live/Dead BacLight™ bacterial viability kit (Invitrogen Life Technologies, Alfagene, Portugal) [37].

This kit differentiates between viable cells (with intact membranes) and dead cells (with damaged membranes) by selective staining using two nucleic acid-binding dyes: SYTO 9™ and propidium iodide (PI). SYTO 9™ penetrates all bacterial membranes, staining the cells green, while PI only stains cells with compromised membranes, producing a red fluorescence. Biofilm cell suspensions were sequentially stained with 250 μL of SYTO 9™ and 50 μL of PI in microcentrifuge tubes. Then, biofilm cell suspensions were filtered through a 0.22 μm Nucleopore® (Whatman, UK) black polycarbonate membrane after 7 min in the dark at room temperature. The membranes were mounted using BacLight™ mounting oil per the manufacturer's guidelines. Sample observations were conducted under a LEICA DMLB2 epifluorescence microscope (LEICA Microsystems, Germany) equipped with a UV light source, 480–500 nm excitation filter, and 485 nm emission filter (Chroma 61,000-V2 DAPI/FITC/TRITC). The images were acquired with a LEICA DFC300 FX camera and LEICA IM50 Image Manager, Image processing, and archiving software. For each sample, 30 fields were analysed to calculate total and non-damaged (viable) cells (cells/cm^2). Data were expressed as log cells/cm^2 for cells with non-damaged membranes. The VBNC cells were calculated by subtracting the culturable cells (CFUs) from the viable cells (non-damaged bacterial cells).

2.5.2. Biofilm structure - optical coherence tomography

Biofilm thickness (μm) and roughness coefficient were evaluated for both non-treated and treated biofilms with chlorine at 5 mg/L for 30 min. Coupons containing biofilms were gently immersed in STW to eliminate suspended cells and to hold the biofilm hydrated. After that, Image acquisition was carried out using a Thorlabs Ganymede spectral domain system (Thorlabs GmbH, Germany) operating at a central wavelength of 930 nm, and biofilm structure analysis was performed through the Biofilm Structure Classification Automatic Processor (BISCAP) as described by Pereira et al. [10]. At least eight 2D OCT images were acquired for each condition and for each independent assay.

2.5.3. Extracellular polymeric substances content

The content of EPS was evaluated in terms of total extracellular protein and polysaccharide concentrations. The extraction of EPS from biofilms was performed using Dowex® Marathon© resin (NA^+ form, strongly acidic, 20–50 mesh, Sigma-Aldrich, Germany) [38], and using the extraction buffer prepared as described by Gomes et al. [35]. After 4 h of extraction at 400 rpm and 4 °C, the EPS content (in the supernatant) was separated from the cells through centrifugation (3700 ×*g*, 5 min) and precipitated with 1:4 ice-cold acetone and stored at −20 °C for 30 min to improve EPS extraction [39]. The resultant solution was then centrifuged at 3700 ×*g* for 10 min, and EPS were resuspended in sterile UPW for quantification. The total extracellular protein concentration was determined following Lowry et al. [40] as modified by Peterson [41], using the Total Protein Kit, Micro Lowry, Peterson's Modification, with bovine serum albumin (BSA) as standard. The concentration of extracellular polysaccharides was quantified using the phenol-sulphuric acid method with glucose as standard [42]. The detection limit (DL) of protein and polysaccharide quantification was 2.9 μg/cm^2 and 2.6 μg/cm^2, respectively.

2.5.4. Confocal laser scanning microscopy analysis

The spatial distribution of EPS components in dual-species biofilms, non-exposed and exposed to MP, 3-Cl-MP, and 3,5-diCl-MP, was evaluated using CLSM combined with multiple fluorescence staining techniques. Bacterial cells were directly stained on PPL coupons using 4′,6-diamidino-2-phenylindole (DAPI - Invitrogen, US) at a final concentration of 0.5 μg/mL for 15 min. After staining, the excess of dye was removed by washing the coupon with sterile distilled water. DAPI is a blue-fluorescent nucleic acid stain that binds to adenine–thymine rich (ATrich) regions of double-stranded deoxyribonucleic acid (DNA) and was used to visualise total bacterial cells [43].

For simultaneous visualization of bacterial cells and polysaccharides in the EPS matrix, samples were first stained for 7 min with 5 μM SYTO 9™ (Invitrogen Life Technologies, Alfagene, Portugal), a cell-permeant fluorescent nucleic acid marker staining the cells green [44]. After removing excess stain, samples were subsequently stained for 1 min with 2 drops of 0.1 % Calcofluor white stain (Sigma-Aldrich, Germany), and then the excess dye was removed again. Calcofluor white stain binds to β(1–3) and β(1,4)-linked polysaccharides present in the bacterial biofilm matrix, especially polysaccharides like cellulose and chitin, staining them blue [45].

Extracellular proteins within the EPS matrix and bacterial cells were also visualised using a combination of FilmTracer SYPRO Ruby (Invitrogen, US) for 30 min, followed by 15 min of DAPI staining. FilmTracer SYPRO Ruby stains a wide range of proteins, including glycoproteins, phosphoproteins, lipoproteins, calcium-binding proteins, and fibrillar proteins, with a magenta colour [46].

Staining protocols were pre-optimised to ensure minimal spectral overlap and enable simultaneous imaging of multiple biofilm components. After staining in the dark and removing excess dye, samples were examined by STELLARIS 5 DM6B-*Z*-CS Confocal Microscope (Leica Microsystems, Germany) at 63× magnification with an oil objective lens with a numerical aperture of 1.40 and refractive index of 1.52 (Leica HC PL APO CS2, Leica Microsystems, Germany). The excitation/emission wavelengths used for image visualization were 405/412–598 nm for DAPI (blue) when used alone. For SYTO 9 ™ (green) and Calcofluor White Stain (blue) in combination, the respective excitation and emission wavelengths were 498/503–676 nm and 405/415–570 nm, respectively. For FilmTracer SYPRO Ruby (red) and DAPI (blue) in combination, the respective excitation and emission wavelengths were 485/512–724 nm and 405/415–570 nm, respectively. Images were obtained through the software Leica Application Suite-Advanced Fluorescence (LAS X, Leica Microsystems GmbH). For each sample, a minimum of six image stacks were acquired in the horizontal plane at a resolution of 512 × 512 pixels, corresponding to a field of view of 387.5 × 387.5 μm. *Z*-stack images were captured with a step size of 1 μm. Three-dimensional (3D) projections of biofilm structures were constructed from the CLSM image acquisitions using the “Easy 3D” tool of IMARIS 9.1 software (Bitplane, Switzerland). Quantitative analysis of biofilm structure, including biovolume ($\mu m^3/\mu m^2$) and surface coverage (%), was carried out using the plug-in COMSTAT2 within the ImageJ software [47]. The biovolume was defined as the volume of biomass (μm^3) from a specific biofilm area divided by the surface area of the substratum (PPL coupons) (μm^2), representing the overall volume of the biofilm, and providing an estimation of the biomass in the biofilm. The surface coverage (%), which is the fraction of the area occupied by biomass in the surface horizontal plane, reflects how efficiently the surface is colonised [47].

2.6. Determination of bacterial susceptibility to antibiotics

The susceptibility of bacteria from non-exposed and MP-, 3-Cl-MP-, and 3,5-diCl-MP-exposed dual-species biofilms was evaluated using the disk diffusion method, following the Clinical and Laboratory Standards Institute (CLSI) guidelines [48]. This approach enables determining whether prior exposure to MP and their transformation products could influence DW bacterial susceptibility to clinically relevant antibiotics. The selected antibiotics, representing different classes recommended by CLSI, were ceftazidime (CEF) at 30 μg/disc; levofloxacin (LEV) at 5 μg/disc; minocycline (MINO) at 30 μg/disc, and trimethoprim-sulfamethoxazole (TMP-SMX) at 1.25/23.75 μg/disc. For that, suspensions of bacterial strain isolated from dual-species biofilms were adjusted to an optical density of 0.135 at 600 nm, equivalent to 0.5 MacFarland standards, and uniformly spread on Mueller-Hinton agar (MHA) plates. Discs with impregnated antibiotics (Oxoid, UK) were placed on the prepared MHA plates, which were then incubated at 37 °C for 24 h. Following incubation, the diameters of the growth inhibition zones were measured and expressed as mean inhibition zone diameters

(mm) ± standard deviation.

2.7. Statistical analysis

GraphPad Prism 8.0 (GraphPad Software, La Jolla California, USA) was used for the statistical analysis of data. The mean and standard deviations (SDs) within samples were calculated using descriptive statistics for all cases based on a minimum of three independent assays, with duplicates. The differences between data were assessed through the one-way analysis of variance ANOVA with Tukey's post-test. Statistical calculations were based on a confidence level of ≥95 % ($P < 0.05$ was considered a statistically significant difference).

3. Results

3.1. Evaluation of MP-chlorinated by-products formation under chlorination

Fourier transform ion cyclotron resonance mass spectra were obtained for UPW and STW, both with and without added MP and free chlorine (Appendix A - Fig. A.1). These spectra form the basis of Fig. 1, enabling precise identification of chlorinated MPs by distinguishing closely related compounds and characterising chlorinated transformation products within complex environmental matrices [14,49–51]. Distinct patterns in the formation of MP-chlorinated by-products were observed following the reaction of MP at 15 µg/L with free chlorine (5 mg/L for 30 min) in UPW and STW, as well as in control samples containing only UPW or STW without MP (Fig. 1). In the absence of MP, no detectable MP-chlorinated by-products were observed in either water type, confirming their formation depends on the presence of MP (Fig. 1 - A). When MP was added, both water types generated the following chlorinated compounds: $C_8H_7ClO_3$ and $C_8H_6Cl_2O_3$, $C_8H_5Cl_3O_3$ and $C_8H_4Cl_4O_3$, corresponding to mono-, di-, tri- and tetra-chlorinated MP, respectively. The formation of these chlorinated by-products involves electrophilic aromatic chlorination, a type of electrophilic substitution reaction where chlorine species (e.g., free chlorine or hypochlorous acid) react with the aromatic ring of MP. This reaction is typical during water disinfection when aromatic compounds are present and is consistent with established mechanisms for chlorinated DBPs formation [52,53].

Comparison between the two water matrices revealed significantly higher signal intensities for MP-chlorinated by-products in STW, with average abundances of $C_8H_6Cl_2O_3$ and $C_8H_5Cl_3O_3$ about 2.93 and 1.4 times higher than in UPW, indicating enhanced reactivity in STW (Fig. 1 - B). These differences suggest that interactions between MP and the chemical constituents of each water type influence the extent and nature of chlorination. Overall, chlorination at 5 mg/L of free chlorine for 30 min in the presence of MP at 15 µg/L results in the formation of mono- to tetra-MP-chlorinated by-products. Proposed reaction pathways are presented in Fig. 1 - C. Additionally, quantification of 3,5-diCl-MP following the reaction of MP at 100 µg/L with free chlorine at 5 mg/L for 30 min showed effective formation of this MP-chlorinated by-product, reaching a concentration of 10 µg/L (Appendix B).

3.2. Effect of MP-chlorinated by-products exposure on bacterial characteristics from dual-species biofilms

3.2.1. Bacterial culturability, cellular density, membrane damage of bacteria, and viable but non-culturable cells

Fig. 2 - A presents the culturability (log CFU/cm^2) of *A. calcoaceticus*, *S. maltophilia*, and the total culturable cells in 7-day-old dual-species biofilms, with and without exposure to MP and MP-chlorinated by-

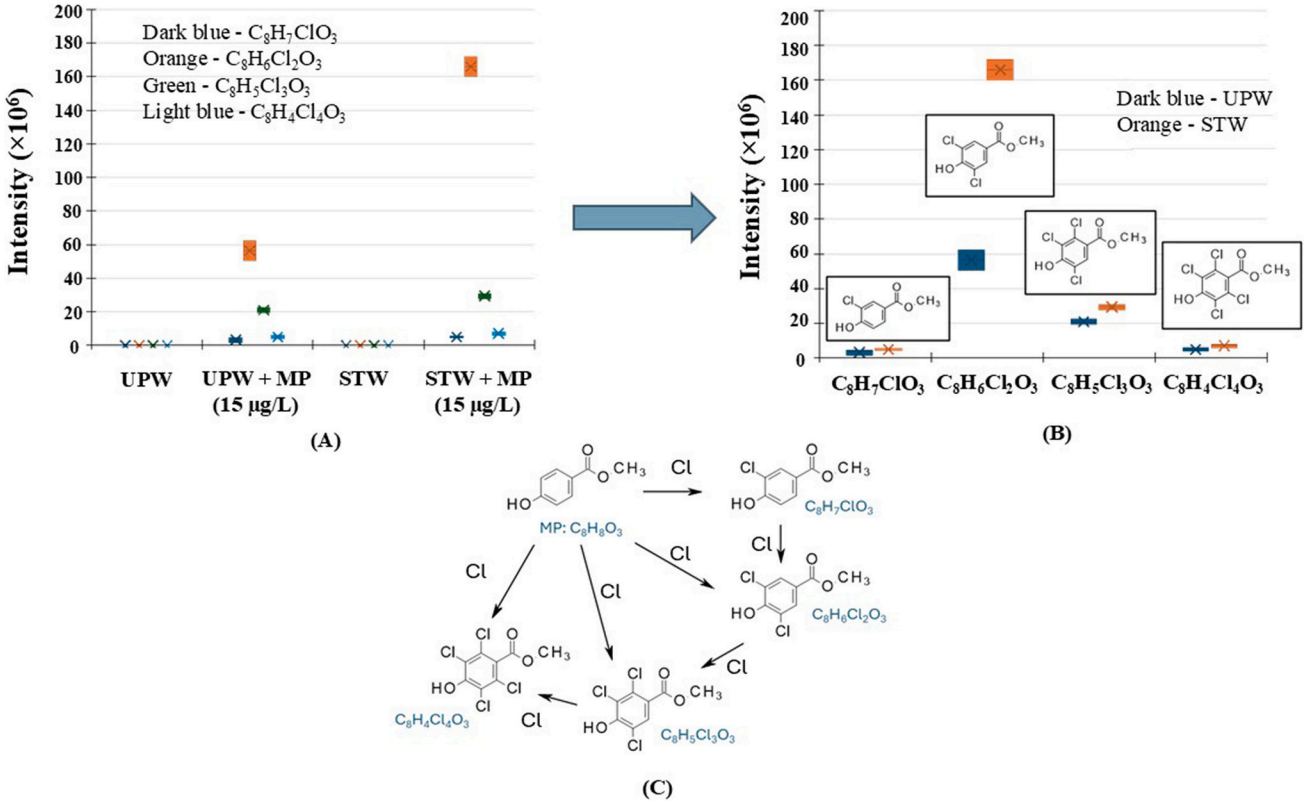

Fig. 1. Ultra-high resolution mass spectrometry (FT-ICR MS) data: (A) Formation levels of MP-chlorinated by-products ($C_8H_7ClO_3$, $C_8H_6Cl_2O_3$, $C_8H_5Cl_3O_3$, and $C_8H_4Cl_4O_3$) after 30 min in UPW, STW, UPW with MP at 15 µg/L, and STW with MP at 15 µg/L, in the presence of 5 mg/L free chlorine. (B) Comparison of peak abundances of these chlorinated compounds formed under identical chlorination conditions (15 µg/L MP and 5 mg/L free chlorine for 30 min) in UPW and STW. (C) A possible formation pathway involving the progressive chlorination of MP leading to these by-products is proposed based on the observed molecular patterns.

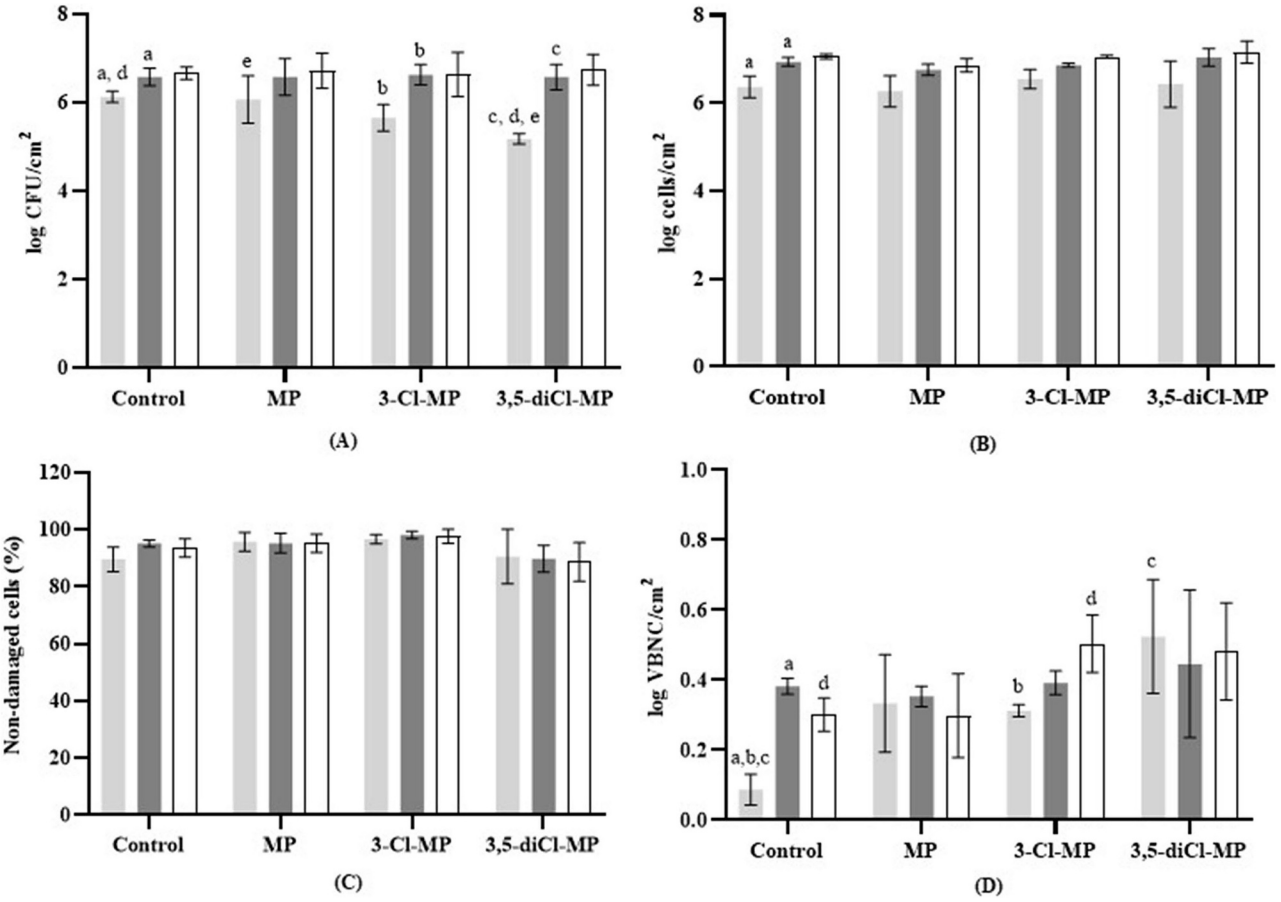

Fig. 2. Characterization of 7-day-old dual-species biofilm cells (▫ *A. calcoaceticus* ▪ *S. maltophilia* □ dual-species biofilms *A. calcoaceticus* + *S. maltophilia*) formed on PPL non-exposed (control – STW) and exposed to MP, 3-Cl-MP, and 3,5-diCl-MP (15 μg/L) in terms of culturability - log CFU/cm^2 (A), total cellular density - log cells/cm^2 (B), percentage of non-damaged cells - % (C), and viable but non-culturable cells - log VBNC cells/cm^2 (D). $^{a, b, c, d, e}$ - correspond to conditions that have statistically significant differences from each other (ANOVA, Tukey's post-hoc test, $P < 0.05$).

products (3-Cl-MP and 3,5-diCl-MP). Across all conditions, *S. maltophilia* exhibited significantly higher culturability than *A. calcoaceticus* in the overall dual-species biofilms. Notably, *S. maltophilia* showed 0.4, 1.0, and 1.4 log CFU/cm^2 more culturable cells than *A. calcoaceticus* in the control, 3-Cl-MP-, and 3,5-diCl-MP- exposed dual-species biofilms, respectively ($P < 0.05$). The culturability of *S. maltophilia* and the overall biofilms were not significantly affected by exposure to MP, 3-Cl-MP, and 3,5-diCl-MP ($P > 0.05$). In contrast, *A. calcoaceticus* within dual-species biofilms showed a significant decrease in culturability (1 log CFU/cm^2) under 3,5-diCl-MP exposure compared to the control ($P < 0.05$). This suggests higher *A. calcoaceticus* susceptibility to 3,5-diCl-MP than *S. maltophilia*. Fig. 2 - B shows the total cell density (log cells/cm^2) of MP-, 3-Cl-MP-, and 3,5-diCl-MP-exposed and non-exposed (control) biofilms. Consistent with culturability data, *S. maltophilia* was more abundant, showing a 0.6 log cells/cm^2 higher cell count than *A. calcoaceticus* in non-exposed (control) biofilms ($P < 0.05$). However, no significant changes in total cell levels were observed in response to MP or MP-chlorinated by-products in either bacterial species or the total biofilm population ($P > 0.05$) - Fig. 2 - B. The percentage of non-damaged cells remained similar across all tested conditions (90–100 %), suggesting that exposure to MP and MP-chlorinated by-products did not significantly affect bacterial membrane integrity ($P > 0.05$) - Fig. 2 - C. The levels of VBNC cells assessed (log VBNC cells/cm^2) are presented in Fig. 2 – D, revealing higher counts for non-exposed *S. maltophilia* compared to non-exposed *A. calcoaceticus* - controls ($P < 0.05$). The exposure to 3-Cl-MP and 3,5-diCl-MP caused a 3-fold and 5-fold increase in the levels of VBNC cells of *A. calcoaceticus* in dual-species biofilms in comparison to non-exposed counterparts, respectively ($P < 0.05$). In contrast, *S. maltophilia* VBNC cell levels remained unaffected by exposure to both MP-chlorinated by-products ($P > 0.05$). This led to a statistically significant increase in total VBNC cells in dual-species biofilms exposed to 3-Cl-MP ($P < 0.05$), whereas the increase observed in 3,5-diCl-MP-exposed biofilms was not significantly different from the control ($P > 0.05$).

3.2.2. Bacterial structure and extracellular polymeric substances composition

Dual-species biofilms exhibited a significant increase in thickness (circa 10 μm) in the presence of 3-Cl-MP compared to non-exposed biofilms ($P < 0.05$). However, the roughness coefficient remained consistent across all tested conditions ($P > 0.05$), as shown in Table 2. Representative OCT images of biofilms formed on PPL coupons are

Table 2
Biofilm thickness (μm), roughness coefficient, and content of EPS (μg/cm^2) obtained for 7-day-old dual-species biofilms non-exposed and exposed to MP, 3-Cl-MP, and 3,5-diCl-MP. *- corresponds to conditions that have statistically significant differences from each other (ANOVA, Tukey's post-hoc test, $P < 0.05$).

	Average thickness (μm)	Roughness coefficient	Proteins (μg/cm^2)	Polysaccharides (μg/cm^2)
Control	20.0 ± 4.1*	0.56 ± 0.11	18.5 ± 0.7	13.0 ± 4.1
MP	26.5 ± 0.5	0.38 ± 0.07	20.6 ± 2.9	13.60 ± 5.3
3-Cl-MP	31.4 ± 1.7*	0.49 ± 0.003	21.8 ± 2.2	21.4 ± 0.2*
3,5-diCl-MP	26.9 ± 5.8	0.48 ± 0.10	22.8 ± 1.3	19.3 ± 2.1*

provided in Appendix C. The content of EPS produced by dual-species biofilms under all experimental conditions were analysed in terms of extracellular proteins and polysaccharides levels (Table 2). The total concentration of proteins was not affected by any compound ($P > 0.05$). However, a significant increase in polysaccharide content was observed for biofilms exposed to 3-Cl-MP and 3,5-diCl-MP ($P < 0.05$) in comparison to non-exposed counterparts.

The biovolume ($\mu m^3/\mu m^2$) and surface coverage (%) of dual-species biofilms, considering polysaccharide and protein components of the EPS matrix, were assessed at the microscale via CLSM analysis (Figs. 3 to 5). Representative CLSM images show that biofilms exposed to 3-Cl-MP and 3,5-diCl-MP formed more dispersed cell aggregates, being more scattered and sparser, compared to the denser structure observed in non-exposed biofilms (Fig. 3 - A to D). Analysis of total bacterial cells, consistent with previous cell density findings, revealed no statistically significant differences in biovolume between control and biofilms exposed to MP, 3-Cl-MP, or 3,5-diCl-MP ($P < 0.05$) - Fig. 3 - E. However, the percentage of surface coverage decreased following exposure to all tested compounds, with the most pronounced effect observed under 3,5-diCl-MP exposure, resulting in an approximate 50 % reduction compared to non-exposed biofilms ($P < 0.05$) - Fig. 3 - F. Images obtained through multiple staining, further demonstrated that biofilms were morphologically heterogeneous, with β-polysaccharides (in blue) - Fig. 4, and proteins (in magenta) - Fig. 5, clearly detectable in all samples. The presence of β-polysaccharides (in blue) occupied a substantial portion of the biofilm matrix across all conditions (Fig. 4 - A to D). Quantitatively, biovolume considering β-polysaccharides and biofilm cells (in green) increased by 2.4- and 4.5-fold in MP- and 3-Cl-MP-exposed biofilms, respectively, compared to non-exposed biofilms ($P < 0.05$) - Fig. 4 - E. In addition, the percentage of surface coverage of EPS associated with β-polysaccharides increased for 3-Cl-MP and 3,5-diCl-MP-exposed biofilms, suggesting increased presence of polysaccharides in the EPS matrix of these biofilms ($P < 0.05$) - Fig. 4 - F. Regarding proteins in the EPS matrix (in magenta), they appear to cover most of biofilm structure (Fig. 5 - A to D). Biofilms exposed to MP- and to 3,5-diCl-MP exhibited higher biovolumes than these non-exposed ($P < 0.05$), with larger structure,s resembling the typical mushrooms-like structure - Fig. 5 - E. Despite this volumetric increase, no statistically significant differences in the percentage of surface coverage were observed between non-exposed and exposed biofilms ($P > 0.05$) - Fig. 5 - F.

3.3. Effect of MP-chlorinated by-products on biofilm tolerance to chlorination: culturability, density, and membrane integrity

As expected, the total reduction of culturable and total cells was not achieved for biofilm cells after free chlorine treatment at 5 mg/L for 30 min. The exposure to MP seems to increase the tolerance of biofilm cells to chlorine at 5 mg/L, as indicated by significantly lower log CFU/cm^2 reduction values for *S. maltophilia* (0.16 ± 0.09) and overall MP-exposed biofilms (0.51 ± 0.09), compared to their non-exposed counterparts (0.66 ± 0.12 and 0.90 ± 0.04, respectively; $P < 0.05$) - Fig. 6 - A. In contrast, biofilms exposed to 3-Cl-MP showed increased susceptibility to chlorine at 5 mg/L. This was reflected in significantly higher log CFU/cm^2 reduction values obtained for *A. calcoaceticus* (1.26 ± 0.07), *S. maltophilia* (1.21 ± 0.14), and overall dual-species biofilms (1.17 ± 0.11) compared to their non-exposed counterparts ($P < 0.05$). On the other hand, exposure to 3,5-diCl-MP did not significantly affect biofilm susceptibility to chlorine, as no notable differences were observed in log reduction values of culturable cells ($P > 0.05$).

Regarding total cell counts, the exposure to MP at 15 μg/L for 7 days did not significantly affect the efficacy of chlorine in reducing the number of total biofilm cells ($P > 0.05$) - Fig. 6 - B. However, biofilms exposed to 3-Cl-MP exhibited significantly higher log cells/cm^2 reductions for *A. calcoaceticus* (0.40 ± 0.03) and overall biofilms (0.32 ± 0.10), compared to non-exposed biofilms (0.20 ± 0.07 and 0.12 ± 0.0005, respectively) ($P < 0.05$) - Fig. 6 - B, suggesting increased susceptibility to chlorine, consistent with previously observed trends in biofilm cells culturability. Similarly, biofilms exposed to 3,5-diCl-MP showed a four-fold higher reduction in total biofilm cells in comparison to the control, after free chlorine treatment at 5 mg/L ($P < 0.05$).

Free chlorine treatment caused about a 20 % decrease in the number of non-damaged cells in non-exposed (control) biofilms. Overall, for biofilms exposed to MP, 3-Cl-MP, and 3,5-diCl-MP, this reduction in biofilm cell viability after chlorine treatment was higher than that observed in the control (Fig. 6 - C). These effects were more pronounced for *S. maltophilia* cells in dual-species biofilms and for the overall dual-species biofilms, with 3-Cl-MP causing the highest decrease in the percentage of non-damaged cells. The percentage of non-damaged cells after chlorination was 38.5 ± 5.9 %, 18.2 ± 1.6 %, and 47.3 ± 4.7 % for MP-, 3-Cl-MP-, and 3,5-diCl-MP-exposed *S. maltophilia* in dual-species biofilms, respectively, whereas non-exposed counterparts showed a percentage of non-damaged cells of 73.3 ± 3.5 % ($P < 0.05$). For the overall dual-species biofilms, the percentage of non-damaged cells was similar and equal to 42.0 ± 6.4 %, 22.0 ± 0.6 %, and 51.8 ± 3.8 % for MP-, 3-Cl-MP-, and 3,5-diCl-MP-exposed dual-species, respectively. Non-exposed dual-species biofilms showed 72.3 ± 3.7 % non-damaged cells ($P < 0.05$). Moreover, MP exposure halved log VBNC cells/cm^2 values for the overall dual-species biofilms, a trend also observed for *A. calcoaceticus* in 3-Cl-MP-exposed biofilms and for *S. maltophilia* and the overall dual-species biofilms under 3,5-diCl-MP exposure ($P < 0.05$) - Fig. 6 - D.

3.4. The impact of MP-chlorinated by-products on biofilm structure and EPS composition during chlorination

Chlorine treatment at 5 mg/L for 30 min caused a decrease in biofilm thickness of approximately 28 % and 47 % on MP- and 3-Cl-MP-exposed dual-species biofilms, respectively, compared to non-treated biofilms. However, no reductions in biofilm thickness were observed after disinfection in non-exposed biofilms (control) and 3,5-diCl-MP-exposed biofilms. Therefore, the exposure to MP and 3-Cl-MP enhances the chlorine action in reducing biofilm thickness. Nonetheless, the thickness of chlorine-treated biofilms did not differ between MP and MP-chlorinated by-products exposure ($P > 0.05$) - Table 3. Representative OCT images of treated biofilms formed on PPL coupons are provided in Appendix D. A decrease of 24 % and 29 % in total protein concentrations was observed after chlorination for 3-Cl-MP- and 3,5-diCl-MP-exposed biofilms, respectively. In contrast, no reduction in protein content was detected for MP-exposed biofilms. This suggests increased chlorine action in disturbing proteins in 3-Cl-MP and 3,5-diCl-MP-exposed biofilms than MP-exposed biofilms or controls. Besides that, chlorine-treated biofilm revealed similar content of proteins and polysaccharides, independently of the exposure to MP and MP-chlorinated by-products ($P > 0.05$) – Table 3. In addition, chlorine treatment did not reduce the polysaccharide in any of the biofilm samples ($P > 0.05$). Although 3-Cl-MP and 3,5-diCl-MP-exposed biofilms showed higher concentrations of polysaccharides, no significant differences were observed after chlorination in comparison to MP-exposed and non-exposed biofilms ($P > 0.05$) - Table 3.

3.5. Effect of methylparaben disinfection by-products exposure on bacterial susceptibility to antibiotics

The exposure to MP, 3-Cl-MP, and 3,5-diCl-MP did not alter the tolerance of *A. calcoaceticus* cells from dual-species biofilms to antibiotics ($P > 0.05$), as shown in Table 4. However, *S. maltophilia* cells from dual-species biofilms appeared more susceptible to MINO and TMP-SMX when growing in the presence of 3,5-diCl-MP, by revealing higher diameters of growth inhibition halos in comparison to non-exposed counterparts ($P < 0.05$) - Table 4.

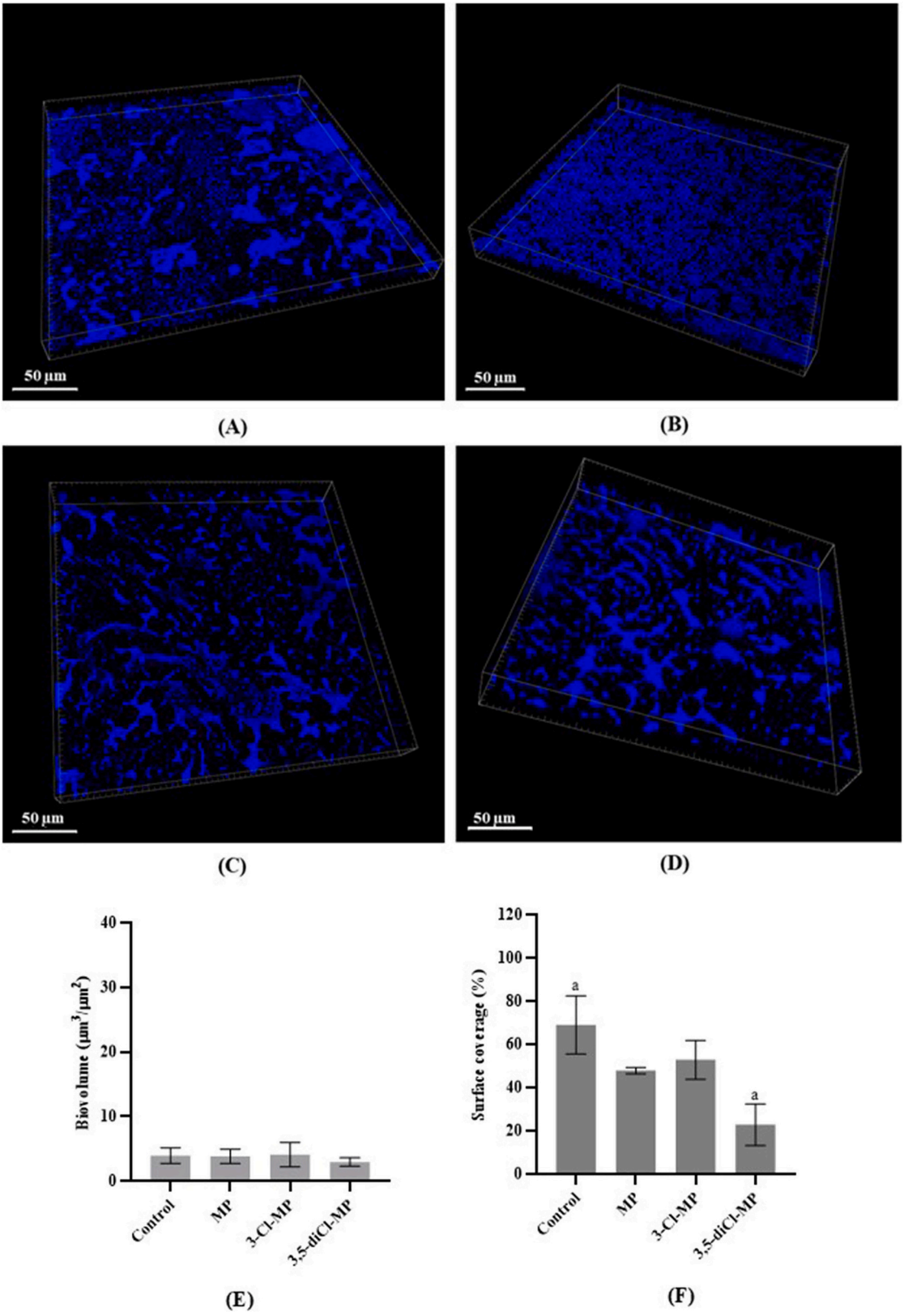

Fig. 3. Representative three-dimensional (3D) confocal images of 7-day-old dual-species biofilms (*A. calcoaceticus* and *S. maltophilia*), non-exposed (A), and exposed to MP (B), 3-Cl-MP (C), and 3,5-diCl-MP (D), stained with DAPI for bacterial cells visualization in blue. The total biovolume ($\mu m^3/\mu m^2$) – E and the percentage of surface coverage by the biofilms (%) – F, for each condition. [a] - samples were statistically different from each other (ANOVA, Tukey's post-hoc test, $P < 0.05$). (For interpretation of the references to colour in this figure legend, the reader is referred to the web version of this article.)

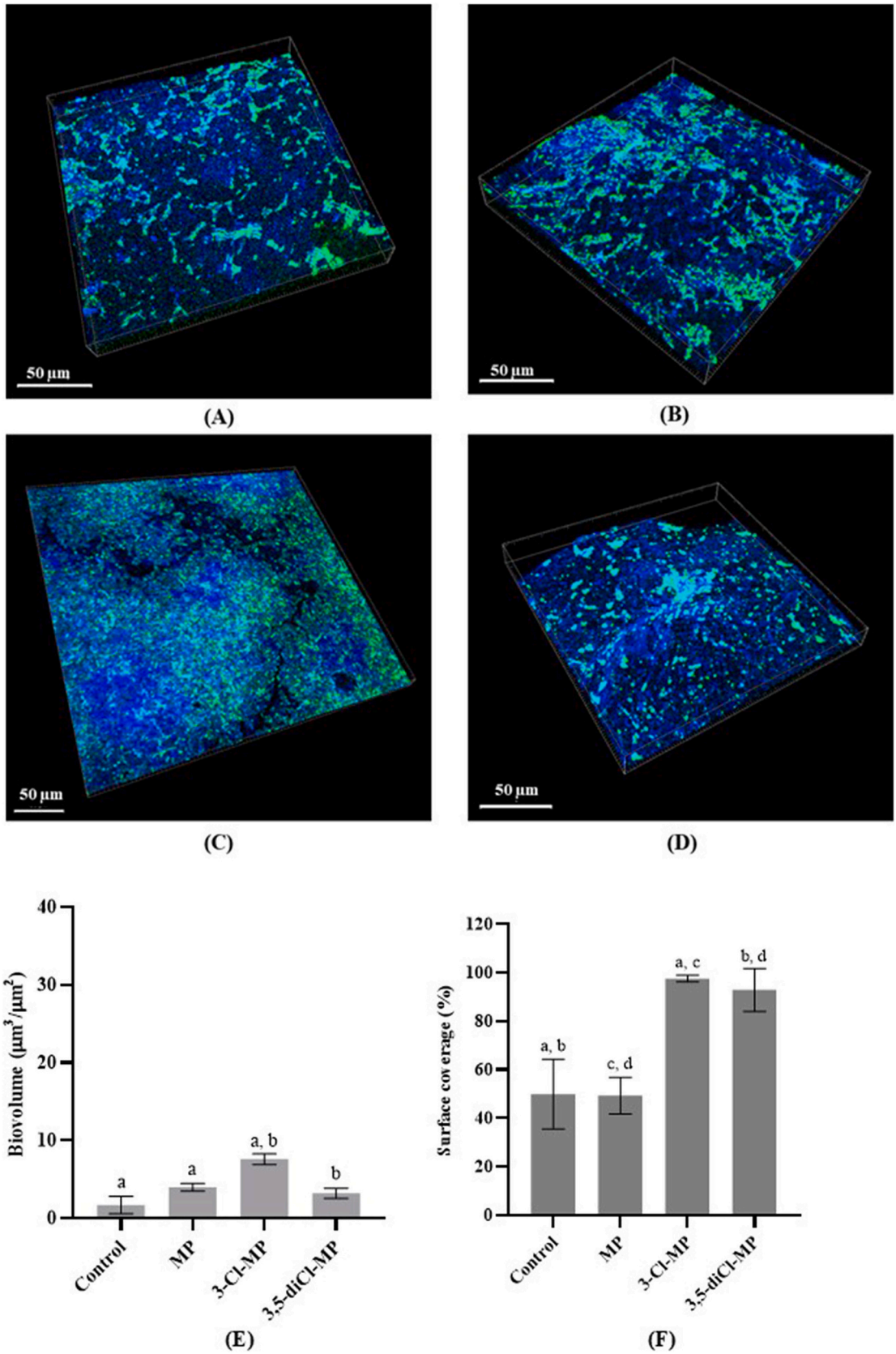

Fig. 4. Representative three-dimensional (3D) confocal images of 7-day-old dual-species biofilms (*A. calcoaceticus* and *S. maltophilia*), non-exposed (A), and exposed to MP (B), 3-Cl-MP (C), and 3,5-diCl-MP (D) stained with Calcofluor White Stain and SYTO 9 for β-polysaccharides (in blue) and bacterial cells (in green) visualization, respectively. The total biovolume ($\mu m^3/\mu m^2$) – E and the percentage of surface coverage by the biofilms (%) – F, for each condition. $^{a, b, c, d}$ - samples were statistically different from each other (ANOVA, Tukey's post-hoc test, $P < 0.05$). (For interpretation of the references to colour in this figure legend, the reader is referred to the web version of this article.)

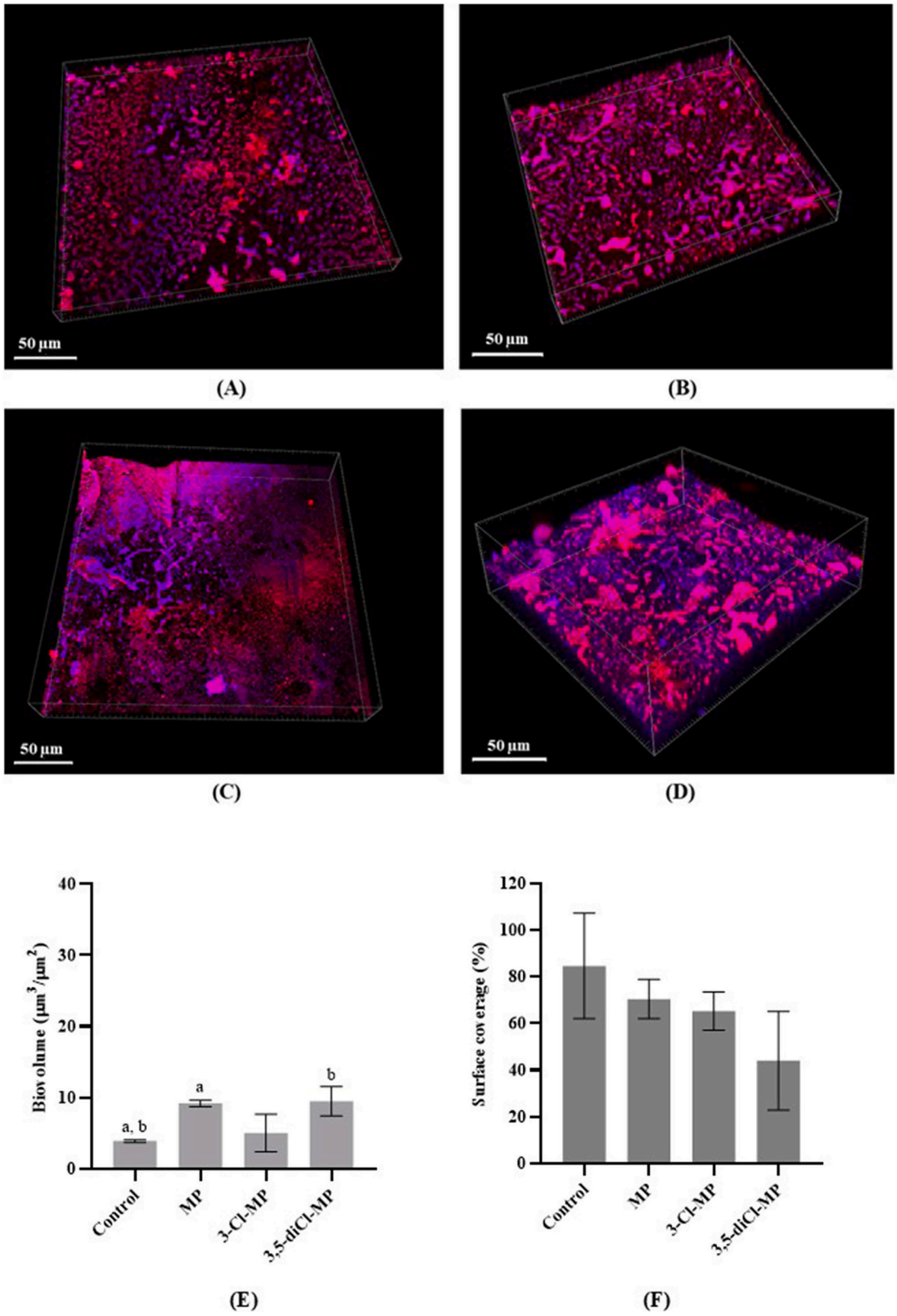

Fig. 5. Representative three-dimensional (3D) confocal images of 7-day-old dual-species biofilms (*A. calcoaceticus* and *S. maltophilia*), non-exposed (A), and exposed to MP (B), 3-Cl-MP (C), and 3,5-diCl-MP (D) stained with FilmTracer SYPRO Ruby and DAPI for proteins (in magenta) and bacterial cells (in blue) visualization, respectively. The total biovolume ($\mu m^3/\mu m^2$) – E and the percentage of surface coverage by the biofilms (%) – F, for each condition. $^{a, b}$ - samples were statistically different from each other (ANOVA, Tukey's post-hoc test, $P < 0.05$). (For interpretation of the references to colour in this figure legend, the reader is referred to the web version of this article.)

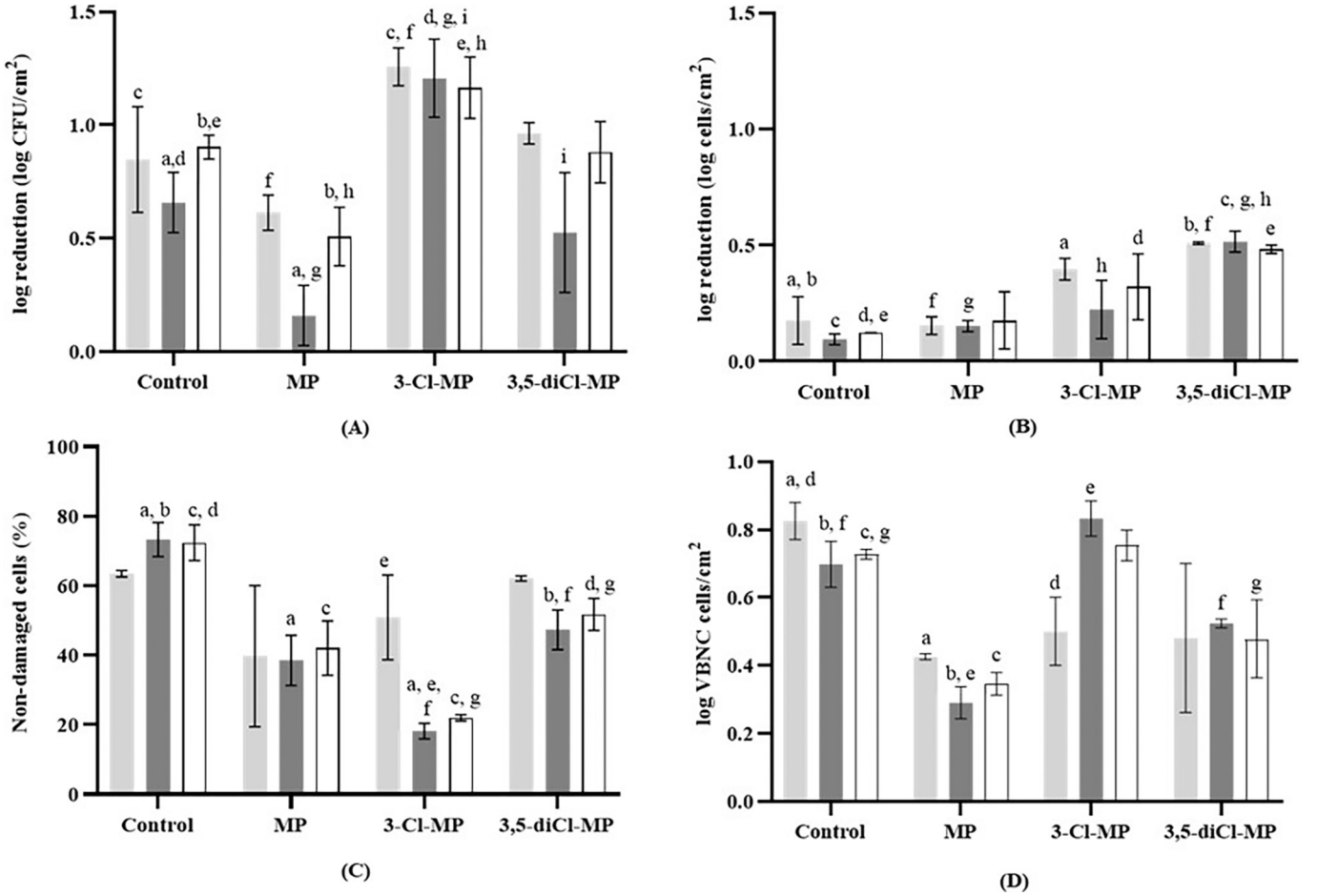

Fig. 6. Logarithmic reduction of culturable cells - log CFU/cm^2 (A), and total cells - log cells/cm^2 (B), characterization of bacterial membrane integrity in terms of non-damaged bacterial cells - % (C) and viable but non-culturable cells - log VBNC cells/cm^2 (D) from non-exposed (control) and exposed to MP, 3-Cl-MP, and 3,5-diCl-MP dual-species biofilms (▫ *A. calcoaceticus* ▪ *S. maltophilia* □ dual-species biofilms *A. calcoaceticus* + *S. maltophilia*) treated with 5 mg/L of free chlorine for 30 min. $^{a, b, c, d, e, f, g, h, i}$ - correspond to conditions that have statistically significant differences from each other (ANOVA, Tukey's post-hoc test, $P < 0.05$).

Table 3
Biofilm thickness (μm), roughness coefficient, and content of EPS (μg/cm^2) obtained for 7-day-old dual-species biofilms, non-exposed and exposed to MP, 3-Cl-MP, and 3,5-diCl-MP after free chlorine treatment at 5 mg/L for 30 min.

	Average thickness (μm)	Roughness coefficient	Proteins (μg/cm^2)	Polysaccharides (μg/cm^2)
Control	19.6 ± 1.5	0.40 ± 0.10	19.9 ± 1.9	17.9 ± 8.2
MP	20.7 ± 1.0	0.40 ± 0.06	18.5 ± 1.8	17.4 ± 6.4
3-Cl-MP	21.3 ± 5.8	0.28 ± 0.12	17.6 ± 0.6	20.7 ± 5.8
3,5-diCl-MP	25.7 ± 4.3	0.53 ± 0.02	17.7 ± 1.4	17.1 ± 2.5

4. Discussion

The formation of 3-Cl-MP and 3,5-diCl-MP when MP at 15 μg/L reacts with free chlorine at 5 mg/L for 30 min was confirmed, demonstrating that parabens can rapidly transform into chlorinated by-products [54,55]. Canosa et al. [54] were the first to show that free chlorine at 0.4 mg/L in tap water can transform parabens into chlorinated by-products in a few minutes. For example, ethylparaben (EP) at 10 μg/L reacted with 0.4 mg/L to form 3-Cl-EP and 3,5-diCl-EP, reaching peak concentrations at 20 and 50 min, respectively [54]. When the chlorine concentration was increased to 5 mg/L, these peaks occurred earlier - at 10 min for 3-Cl-EP and 25 min for 3,5-diCl-EP - with 3-Cl-EP

Table 4
Inhibition halos (mm) obtained for bacteria isolated from 7-day-old dual-species biofilms, non-exposed (control) and exposed to MP, 3-Cl-MP, and 3,5-diCl-MP. All used antibiotic discs measured 6 mm. *- samples were statistically different from their respective non-exposed biofilms – control (ANOVA, Tukey's post-hoc test, $P < 0.05$).

	Antibiotics	CEF (30 μg/disc)	LEV (5 μg/disc)	MINO (30 μg/disc)	TMP-SMX (1.25/23.75 μg/disc)
A. calcoaceticus	Control	20.3 ± 0.5	29.5 ± 0.4	29.6 ± 0.3	20.1 ± 0.8
	MP	21.0 ± 0.4	31.0 ± 1.6	32.7 ± 2.5	21.3 ± 0.3
	3-Cl-MP	20.6 ± 0.3	29.1 ± 2.0	30.7 ± 1.3	19.9 ± 0.7
	3,5-diCl-MP	20.5 ± 1.8	29.9 ± 0.8	30.8 ± 0.8	19.3 ± 0.7
S. maltophilia	Control	13.9 ± 1.3	32.1 ± 0.5	32.8 ± 0.9*	14.4 ± 0.9*
	MP	13.0 ± 0.7	33.0 ± 2.8	35.3 ± 1.9	16.0 ± 1.1
	3-Cl-MP	14.3 ± 0.9	31.8 ± 0.1	33.7 ± 1.2	14.7 ± 1.7
	3,5-diCl-MP	16.8 ± 2.3	32.8 ± 2.6	35.9 ± 0.1*	17.5 ± 1.0*

disappearing by 25 min. The persistence of 3,5-diCl-EP up to 180 min suggests that 3-Cl-EP is further transformed into 3,5-diCl-EP, and that di-chlorinated by-products are more resistant to further oxidation [54]. Similarly, Terasaki et al. [55] observed the formation of chlorinated derivatives from parabens in tap water, noting a rapid increase in mono-chlorinated propylparaben (3-Cl-PP) within the first 2.5 min, followed by a decrease, resulting in the presence of di-chlorinated PP (3,5-diCl-PP) due to further chlorination.

The findings suggested that the presence of 3,5-diCl-MP reduced the culturability of *A. calcoaceticus* presented in 7-day dual-species biofilms, highlighting the stronger effect of a di-halogenated compound in relation to a mono-halogenated one [56], and the more susceptible profile of *A. calcoaceticus* to environmental stress conditions in comparison to *S. maltophilia.* Other studies have also indicated that di-halogenated compounds have greater toxicity (to animal and plant cells) than mono-halogenated parabens [57–59]. Confocal analysis also revealed a 50 % decrease in biofilm coverage for 3,5-diCl-MP-exposed dual-species biofilms that may be related to the decreased culturability of *A. calcoaceticus*. This may be attributed to oxidative stress caused by chlorinated compounds, leading to a compromised membrane integrity [60,61]. To further study this effect, bacterial cell replication parameters were evaluated (Appendix E). These analyses showed a reduction in the A_{max} values for *A. calcoaceticus*, indicating suppressed cell growth in the presence of MP-chlorinated by-products. In addition, extended lag phases (λ) were shown for *S. maltophilia* when these compounds were presented, suggesting an adaptive response to the stress they induced (Appendix E). Although 3,5-diCl-MP reduced *A. calcoaceticus* culturability, its exposure increases the number of *A. calcoaceticus* VBNC cells, as observed for 3-Cl-MP-exposed *S. maltophilia* and consequently for the overall cells in the dual-species biofilms. An increase in the number of VBNC cells may indicate the dormant state adoption of bacterial cells in biofilms, which has been associated with a more tolerant state to stressful conditions and external factors [62]. Under VBNC state, bacteria retain their metabolic activity and pathogenicity but not culturability [63]. These cells can continuously metabolise, accumulate, and secrete EPS precursors with different functional groups, including proteins, polysaccharides, and fatty acids [64]. Nevertheless, their metabolic activity is generally lower than that of culturable cells [63]. Consistent with this, a previous study reported that bacterial cells exposed to parabens exhibited reduced metabolic activity, proposing that exposure to parabens and their chlorinated by-products may induce stress responses that drive cells into a dormant (VBNC) state [11].

Environmental contaminants may also cause microorganisms to modify their EPS components, such as changing the ratio of polysaccharides and proteins, and the spatial distribution of EPS, to adapt to environmental conditions [64,65]. An increase in biofilm thickness and polysaccharide concentration in the EPS matrix was observed for 3-Cl-MP-exposed dual-species biofilms. This increase in biofilm thickness was mainly attributed to an enhanced polysaccharide production rather than biofilm cell proliferation. Indeed, CLSM analysis showed similar biovolumes and percentages of surface coverage by cells in 3-Cl-MP–exposed and non-exposed biofilms, whereas Calcofluor staining revealed greater biovolume and surface coverage by polysaccharides in the matrix of 3-Cl-MP-exposed biofilms. The increased content of polysaccharides in the EPS matrix may result in a heterogeneous structure with denser and thicker clusters, justifying the increased thickness when biofilms were formed in the presence of 3-Cl-MP. Dual-species biofilms exposed to 3,5-diCl-MP also revealed twice the polysaccharide content in comparison to the control, with CLSM analysis revealing a higher percentage of biofilm surface coverage by polysaccharides. Increased polysaccharide content suggested that the protective mechanism of EPS might be stimulated to maintain the stability of the biofilm [66]. Indeed, polysaccharides in the EPS matrix play a crucial role in increasing biofilm strength and rigidity, increasing the integrity and stability of the biofilm skeleton [67,68]. Other authors have also shown that subinhibitory exposure to environmental contaminants such as heavy metals - mercury [69], musks - tonalide [70], antibiotics - sulfadiazine and ciprofloxacin [71], and *per*- and polyfluoroalkyl substances (PFAS) [72,73], induces biofilm formation by potentiating the increase of EPS. Overall, chlorinated by-products seem to induce bacterial adaptive responses across molecular, cellular, and community levels, leading to stress-related growth reduction, changes in EPS production, and altered biofilm architecture. Changes in biofilm matrix composition may affect the chlorination efficacy in water disinfection since biofilms with enriched EPS (polysaccharides and proteins) exhibit stronger structural integrity, viscoelasticity, and surface adherence [74,75]. These properties make biofilms more difficult to control and eliminate due to enhanced mechanical strength and shear stress resistance [74]. In addition, residual chlorine can interact with the EPS matrix, reducing its availability and thus protecting internal microorganisms [76,77]. Furthermore, the EPS components, as sources of organic matter, can react with chlorine, potentiating the formation of DBPs, thereby compromising DW safety due to the presence of these hazardous compounds [64].

Lower log CFU/cm^2 reductions were observed in MP-exposed *S. maltophilia* and overall biofilm cells compared to those not exposed, suggesting increased tolerance to disinfection in the presence of MP. This effect was previously reported by Pereira and Gomes [12] for the same compound at 15 μg/L against the same bacterial strains. It has also been shown that the presence of MP increases biofilm cell proliferation and biofilm thickness [10], suggesting that MP can serve as a carbon source in water environments [33]. Furthermore, selective pressures from chlorination may allow surviving bacterial cells to utilise microbial decay products from disinfection-inactivated microorganisms, as well as other carbon sources such as parabens, leading to increased bacterial cell proliferation [78]. Similarly, trace antibiotics were found to reduce biofilm inactivation rates in DWDSs after chlorination compared to controls, indicating enhanced chlorine resistance [79].

Although the polysaccharide content was not affected by chlorination among different biofilms, higher reductions in biofilm thickness after chlorination were observed for MP- and 3-Cl-MP-exposed dual-species biofilms compared to the control. Similarly, increased reductions in protein content were observed in 3-Cl-MP- and 3,5-di-Cl-MP-exposed dual-species biofilms in comparison to non-exposed biofilms. This suggests increased chlorine efficacy in disturbing biofilm structure and EPS composition when these compounds are present, which is surprising given that biofilms grown with 3-Cl-MP and 3,5-diCl-MP appeared to have stronger integrity than the non-exposed control biofilms. However, the simultaneous reduction in protein content and biofilm thickness may also explain the higher log reductions observed in both culturable and total cell counts, and the reduction in the percentage of non-damaged cells in biofilms exposed to MP-chlorinated by-products. This suggests that chlorine more effectively penetrated and disrupted the EPS matrix of MP-chlorinated by-products, enhancing its impact on bacterial cells. Consequently, exposure to these by-products increases bacterial biofilm susceptibility to chlorine. Overall, whereas MP indirectly enhances chlorine tolerance by boosting biofilm growth, chlorinated by-products act as stress agents, limiting cell growth and making biofilms more vulnerable to chlorine, even if EPS production rises as an apparent partial protective response.

In general, DBPs are reported to induce bacterial antibiotic resistance, as higher levels of antibiotic-resistant bacteria (ARB) are found in disinfected DW compared to raw water [22]. Therefore, in this study, the antibiotic susceptibility of bacterial cells from biofilms grown in the presence of MP and by-products was evaluated. This is important from a public health perspective, since bacteria originating from DWDSs may opportunistically colonize susceptible hosts (e.g., immunocompromised patients), facing different therapeutic antibiotic treatments. Curiously, increased bacterial susceptibility to antibiotics (MINO and TMP-SMX) was observed for 3,5-diCl-MP-exposed *S. maltophilia* cells in dual-species biofilms in relation to non-exposed counterparts. However, further research is needed to investigate at the molecular level changes in ARG expression induced by PTP exposure. Other studies showed that

environmental contaminants can increase bacterial susceptibility to antibiotics [80], although such findings are less common compared to those reporting increased antibiotic resistance, in particular, from parabens exposure [81–83]. An important factor to consider is the duration of exposure to these environmental contaminants that may influence shifts in bacterial resistance profiles. For example, Rabow et al. [84] studied the effects of copper pollution on soil bacterial communities and found that while long-term copper exposure generally increased bacterial resistance to both copper and tetracycline, short-term laboratory experiments decreased bacterial resistance to tetracycline. This work raises concerns about the environmental release of PTP that impacts microbial communities in unexpected ways as well as the human health. However, further research at the molecular-level is needed to understand the mechanisms underlying the observed cellular and community-level changes. In addition, continuous-flow and multi-species biofilm studies will further help understanding the impact of parabens and their transformation products on DW microbial communities.

5. Conclusions

Biofilms grown with 3,5-diCl-MP showed reduced culturability, and 3-Cl-MP- and 3,5-diCl-MP-exposed biofilms appeared to enter a VBNC state. These results suggest that MP-chlorinated by-products may promote dormancy in DW biofilm cells. These cellular adaptations were further reflected in structural modifications. Biofilms exposed to 3-Cl-MP were about 10 μm thicker than these non-exposed, and both PTP exposure altered EPS production as a protective response. On the opposite, PTP induced stress responses in the DW biofilms, making them more susceptible to chlorine. Indeed, 3-Cl-MP and 3,5-diCl-MP-exposed dual-species biofilms showed had lower numbers of culturable and total cell, accompanied by a decrease in the percentage of non-damaged cells. Chlorine treatment also caused protein loss and reduced the thickness of PTP-exposed biofilms. Moreover, 3,5-diCl-MP exposure increased *S. maltophilia* susceptibility to MINO and TMP-SMX, showing that PTP influenced bacterial response to antibiotics. Overall, the presence of PTP in DW affected the growth and behavior of biofilms present in these ecosystems, with potential impact to the public health.

CRediT authorship contribution statement

Ana Rita Pereira: Writing – original draft, Visualization, Methodology, Investigation, Data curation, Conceptualization. **Inês B. Gomes:** Writing – review & editing, Visualization, Validation, Supervision, Methodology, Formal analysis, Data curation, Conceptualization. **Mourad Harir:** Writing – review & editing, Visualization, Validation, Methodology, Investigation. **Ana R.L. Ribeiro:** Writing – review & editing, Visualization, Validation, Methodology, Investigation. **Ana M. Gorito:** Writing – review & editing, Visualization, Validation, Methodology, Investigation. **Lúcia Santos:** Writing – review & editing, Visualization, Validation, Supervision, Methodology, Investigation. **Manuel Simões:** Writing – review & editing, Visualization, Validation, Supervision, Software, Resources, Project administration, Methodology, Formal analysis, Conceptualization.

Declaration of competing interest

The authors declare that they have no known competing financial interests or personal relationships that could have appeared to influence the work reported in this paper.

Acknowledgements

This work was supported by national funds through FCT/MCTES (PIDDAC): LEPABE, UIDB/00511/2020 (DOI: 10.54499/UIDB/ 00511/ 2020) and UIDP/00511/2020 (DOI: 10.54499/UIDP/00511/ 2020) and ALiCE, LA/P/0045/2020 (DOI: 10.54499/LA/P/0045/ 2020); Project InnovAntiBiofilm (ref. 101157363) financed by the European Commission (Horizon-Widera 2023-Acess-02/Horizon-CSA); FEDER funds through the Operational Programme Competitiveness Factors-COMPETE, and national funds by the Foundation for Science and Technology (FCT) under research grant HCAI_Disinfect (ref. COMPETE2030-FEDER-00752300; N° 16360); Ana Rita Pereira's PhD scholarship by 2021.06226.BD (DOI: 10.54499/2021.06226.BD) and Inês B. Gomes contract 2022.06488.CEECIND/ CP1733/CT0008 (DOI: 10.54499/2022.06488.CEECIND/CP1733/ CT0008) both provided by FCT. A.M.G. and A.R.L.R. acknowledge the support from FCT, I.P. /MCTES through national funds: LSRE-LCM, UID/50020. ARLR acknowledges the support from FCT funding under the Scientific Employment Stimulus - Individual Call (DOI: 10.54499/2022.00184.CEECIND/CP1733/CT0001).

Appendix A. Supplementary data

Supplementary data to this article can be found online at https://doi.org/10.1016/j.jwpe.2025.109061.

Data availability

Data will be made available on request.

References

[1] A.R. Pereira, M. Simões, I.B. Gomes, Parabens as environmental contaminants of aquatic systems affecting water quality and microbial dynamics, Sci. Total Environ. 905 (2023), https://doi.org/10.1016/j.scitotenv.2023.167332.
[2] F. Wei, M. Mortimer, H. Cheng, N. Sang, L.H. Guo, Parabens as chemicals of emerging concern in the environment and humans: a review, Sci. Total Environ. 778 (2021), https://doi.org/10.1016/j.scitotenv.2021.146150.
[3] C.W. Pai, D. Leong, C.Y. Chen, G.S. Wang, Occurrences of pharmaceuticals and personal care products in the drinking water of Taiwan and their removal in conventional water treatment processes, Chemosphere 256 (2020), https://doi.org/10.1016/j.chemosphere.2020.127002.
[4] E.K. Radwan, M.B.M. Ibrahim, A. Adel, M. Farouk, The occurrence and risk assessment of phenolic endocrine-disrupting chemicals in Egypt's drinking and source water, Environ. Sci. Pollut. Res. 27 (2020) 1776–1788, https://doi.org/10.1007/s11356-019-06887-0.
[5] J. Lincho, R.C. Martins, J. Gomes, Paraben compounds—part i: an overview of their characteristics, detection, and impacts, Appl. Sci. (Switzerland) 11 (2021) 1–38, https://doi.org/10.3390/app11052307.
[6] X. Xue, J. Xue, W. Liu, D.H. Adams, K. Kannan, Trophic magnification of parabens and their metabolites in a subtropical marine food web, Environ. Sci. Technol. 51 (2017) 780–789, https://doi.org/10.1021/acs.est.6b05501.
[7] E.I. Prest, F. Hammes, M.C.M. van Loosdrecht, J.S. Vrouwenvelder, Biological stability of drinking water: controlling factors, methods, and challenges, Front. Microbiol. 7 (2016), https://doi.org/10.3389/fmicb.2016.00045.
[8] H. Bin Wang, Y.H. Wu, L.W. Luo, T. Yu, A. Xu, S. Xue, G.Q. Chen, X.Y. Ni, L. Peng, Z. Chen, Y.H. Wang, X. Tong, Y. Bai, Y.Q. Xu, H.Y. Hu, Risks, characteristics, and control strategies of disinfection-residual-bacteria (DRB) from the perspective of microbial community structure, Water Res. 204 (2021), https://doi.org/10.1016/j.watres.2021.117606.
[9] K. Sauer, P. Stoodley, D.M. Goeres, L. Hall-Stoodley, M. Burmølle, P.S. Stewart, T. Bjarnsholt, The biofilm life cycle: expanding the conceptual model of biofilm formation, Nat. Rev. Microbiol. 20 (2022) 608–620, https://doi.org/10.1038/s41579-022-00767-0.
[10] A.R. Pereira, I.B. Gomes, M. Simões, Impact of parabens on drinking water bacteria and their biofilms: the role of exposure time and substrate materials, J. Environ. Manag. 332 (2023) 117413, https://doi.org/10.1016/j.jenvman.2023.117413.
[11] A.R. Pereira, I.B. Gomes, M. Simões, Parabens alter the surface characteristics and antibiotic susceptibility of drinking water bacteria, Chemosphere 368 (2024) 143704, https://doi.org/10.1016/j.chemosphere.2024.143704.
[12] A.R. Pereira, I.B. Gomes, The effects of methylparaben exposure on biofilm tolerance to chlorine disinfection, J. Hazard. Mater. (2024) 134883, https://doi.org/10.1016/j.jhazmat.2024.134883.
[13] M.T. Penrose, G.P. Cobb, Identifying potential paraben transformation products and evaluating changes in toxicity as a result of transformation, Water Environ. Res. 94 (2022), https://doi.org/10.1002/wer.10705.
[14] C. Postigo, R. Gil-Solsona, M.F. Herrera-Batista, P. Gago-Ferrero, N. Alygizakis, L. Ahrens, K. Wiberg, A step forward in the detection of byproducts of anthropogenic organic micropollutants in chlorinated water, Tren. Environ. Anal. Chem. 32 (2021) e00148, https://doi.org/10.1016/j.teac.2021.e00148.
[15] W. Wang, K. Kannan, Fate of parabens and their metabolites in two wastewater treatment plants in New York State, United States, Environ. Sci. Technol. 50 (2016) 1174–1181, https://doi.org/10.1021/acs.est.5b05516.

[16] W.L. Chen, Y.S. Ling, D.J.H. Lee, X.Q. Lin, Z.Y. Chen, H.T. Liao, Targeted profiling of chlorinated transformation products and the parent micropollutants in the aquatic environment: a comparison between two coastal cities, Chemosphere 242 (2020), https://doi.org/10.1016/j.chemosphere.2019.125268.
[17] M. Albouy, Y. Deceuninck, V. Migeot, M. Doumas, A. Dupuis, N. Venisse, P. P. Engene, B. Veyrand, T. Geny, P. Marchand, B. Le Bizec, E. Bichon, P. Carato, Characterization of pregnant women exposure to halogenated parabens and bisphenols through water consumption, J. Hazard. Mater. 448 (2023), https://doi.org/10.1016/j.jhazmat.2023.130945.
[18] W. Li, Y. Shi, L. Gao, J. Liu, Y. Cai, Occurrence and human exposure of parabens and their chlorinated derivatives in swimming pools, Environ. Sci. Pollut. Res. 22 (2015) 17987–17997, https://doi.org/10.1007/s11356-015-5050-1.
[19] M.T. Penrose, G.P. Cobb, Evaluating seasonal differences in paraben transformation at two different wastewater treatment plants in Texas and comparing parent compound transformation to byproduct formation, Water Res. 235 (2023), https://doi.org/10.1016/j.watres.2023.119798.
[20] A.R. Pereira, I.B. Gomes, M. Harir, L. Santos, M. Simões, Parabens transformation products in water and their (eco)toxicological implications, Chem. Eng. J. 498 (2024), https://doi.org/10.1016/j.cej.2024.155129.
[21] J.J. Wang, X. Liu, T.W. Ng, J.W. Xiao, A.T. Chow, P.K. Wong, Disinfection byproduct formation from chlorination of pure bacterial cells and pipeline biofilms, Water Res. 47 (2013) 2701–2709, https://doi.org/10.1016/j.watres.2013.02.038.
[22] D. Li, S. Zeng, M. He, A.Z. Gu, Water disinfection byproducts induce antibiotic resistance-role of environmental pollutants in resistance phenomena, Environ. Sci. Technol. 50 (2016) 3193–3201, https://doi.org/10.1021/acs.est.5b05113.
[23] Q. Xiao, X. Xu, L. Chen, B. Fu, J. Cao, J. Liu, H. Zhang, S. Lu, Parabens, triclosan, and triclocarban in aquatic products from Shenzhen, China and the relative health risk, Chemosphere 367 (2024), https://doi.org/10.1016/j.chemosphere.2024.143652.
[24] H. Yoom, J. Shin, J. Ra, H. Son, D. Ryu, C. Kim, Y. Lee, Transformation of methylparaben during water chlorination: effects of bromide and dissolved organic matter on reaction kinetics and transformation pathways, Sci. Total Environ. 634 (2018) 677–686, https://doi.org/10.1016/j.scitotenv.2018.03.330.
[25] N.B. Bolujoko, O.O. Ogunlaja, M.O. Alfred, D.M. Okewole, A. Ogunlaja, O. D. Olukanni, T.A.M. Msagati, E.I. Unuabonah, Occurrence and human exposure assessment of parabens in water sources in Osun State, Nigeria, Sci. Total Environ. 814 (2022), https://doi.org/10.1016/j.scitotenv.2021.152448.
[26] I. Haddaoui, J. Mateo-Sagasta, A review on occurrence of emerging pollutants in waters of the MENA region, Environ. Sci. Pollut. Res. 28 (2021) 68090–68110, https://doi.org/10.1007/s11356-021-16558-8.
[27] L.C. Simões, M. Simões, R. Oliveira, M.J. Vieira, Potential of the adhesion of bacteria isolated from drinking water to materials, J. Basic Microbiol. 47 (2007) 174–183, https://doi.org/10.1002/jobm.200610224.
[28] R.I. Amoli, J. Nowroozi, A. Sabokbar, S. Fattahi, G. Amirbozorgi, Isolation of *Stenotrophomonas maltophilia* from water and water tap, Biomed. Res. 28 (2017) 8750–8754. www.biomedres.info.
[29] J.S. Glover, T.D. Ticer, M.A. Engevik, Profiling antibiotic resistance in *Acinetobacter calcoaceticus*, Antibiotics 11 (2022), https://doi.org/10.3390/antibiotics11070978.
[30] L.C. Simões, M. Simões, M.J. Vieira, Intergeneric coaggregation among drinking water bacteria: evidence of a role for *Acinetobacter calcoaceticus* as a bridging bacterium, Appl. Environ. Microbiol. 74 (2008) 1259–1263, https://doi.org/10.1128/AEM.01747-07.
[31] I. Gomes, L.C. Simões, M. Simões, The effects of emerging environmental contaminants on *Stenotrophomonas maltophilia* isolated from drinking water in planktonic and sessile states, Sci. Total Environ. 643 (2018) 1348–1356, https://doi.org/10.1016/j.scitotenv.2018.06.263.
[32] P.S. Stewart, M.J. Franklin, Physiological heterogeneity in biofilms, Nat. Rev. Microbiol. 6 (2008) 199–210, https://doi.org/10.1038/nrmicro1838.
[33] A.R. Pereira, I.B. Gomes, L. Santos, M. Simões, Track of methylparaben in the bulk phase and on the extracellular matrix of dual-species biofilms: biodegradation and bioaccumulation, J. Hazard. Mater. 480 (2024), https://doi.org/10.1016/j.jhazmat.2024.136222.
[34] WHO, Guidelines for Drinking-water Quality Fourth Edition Incorporating the First Addendum, 4th ed., 2022. https://www.who.int/publications/i/item/9789240045064 (accessed December 19, 2024).
[35] I. Gomes, L. Simões, M. Simões, Influence of surface copper content on *Stenotrophomonas maltophilia* biofilm control using chlorine and mechanical stress, Biofouling 36 (2020) 1–13, https://doi.org/10.1080/08927014.2019.1708334.
[36] I. Gomes, M. Simões, L.C. Simões, The effects of sodium hypochlorite against selected drinking water-isolated bacteria in planktonic and sessile states, Sci. Total Environ. 565 (2016) 40–48, https://doi.org/10.1016/j.scitotenv.2016.04.136.
[37] I. Gomes, M.M. Querido, J.P. Teixeira, C.C. Pereira, L.C. Simões, M. Simões, Prolonged exposure of *Stenotrophomonas maltophilia* biofilms to trace levels of clofibric acid alters antimicrobial tolerance and virulence, Chemosphere 235 (2019) 327–335, https://doi.org/10.1016/j.chemosphere.2019.06.184.
[38] B.O. Frølund, R. Palmgren, K. Keiding, E.R. Nielsen, Extraction of extracellular polymers from activated sludge using a cation exchange resin, Water Res. 30 (1996) 1749–1758, https://doi.org/10.1016/0043-1354(95)00323-1.
[39] A.F. Silva, G. Carvalho, R. Soares, A.v. Coelho, M.T.B. Crespo, Step-by-step strategy for protein enrichment and proteome characterisation of extracellular polymeric substances in wastewater treatment systems, Appl. Microbiol. Biotechnol. 95 (2012) 767–776, https://doi.org/10.1007/s00253-012-4157-2.
[40] O.H. Lowry, N.J. Rosebrough, A.L. Farr, R.J. Randall, Protein measurement with the Folin phenol reagent, J. Biol. Chem. 193 (1951) 265–275.
[41] R.L. Gary Peterson, Review of the folin phenol protein quantitation method of Lowry, Rosebrough, Farr and Randall, Anal. Biochem. 100 (1979) 201–220.
[42] M. Dubois, K. Gilles, J.K. Hamilton, P.A. Rebers, F. Smith, A Colorimetric Method for the Determination of Sugars, Dreywood, R., Indust. Enq. Chem., Anal. Ed vol. 18, 1951, p. 476.
[43] T. Tartari, C. Estrela, L.B.B. de Araújo, M.S.Z. Graeff, F.B. de Andrade, M.A. H. Duarte, Use of confocal laser scanning microscopy to evaluate the metal ion removal and destabilization of *Enterococcus faecalis* biofilms by EDTA and etidronic acid, Odontology (2025), https://doi.org/10.1007/s10266-025-01082-9.
[44] A.R. Silva, D.A.C. Narciso, L.C. Gomes, F.G. Martins, L.F. Melo, A. Pereira, Proof-of-concept approach to assess the impact of thermal disinfection on biofilm structure in hot water networks, J. Water Process Eng. 53 (2023), https://doi.org/10.1016/j.jwpe.2023.103595.
[45] Z.H. Khoury, T. Vila, T.R. Puthran, A.S. Sultan, D. Montelongo-Jauregui, M.A. S. Melo, M.A. Jabra-Rizk, The role of *Candida albicans* secreted polysaccharides in augmenting *Streptococcus mutans* adherence and mixed biofilm formation: *in vitro* and *in vivo* studies, Front. Microbiol. 11 (2020), https://doi.org/10.3389/fmicb.2020.00307.
[46] S. Bie, H. Yuan, C. Shi, C. Li, M. Lu, Z. Yao, R. Liu, D. Lu, T. Ma, H. Yu, Antibiofilm activity of Plumbagin against *Staphylococcus aureus*, Sci. Rep. 15 (2025), https://doi.org/10.1038/s41598-025-92435-5.
[47] A. Heydorn, A.T. Nielsen, M. Hentzer, C. Sternberg, M. Givskov, B.K. Ersbøll, S. Molin, Quantification of Biofilm Structures by the Novel Computer Program COMSTAT. www.im.dtu.dk, 2000.
[48] CLSI, M100-S25 Performance Standards for Antimicrobial Susceptibility Testing; Twenty-Fifth Informational Supplement vol. 35, 2015. www.clsi.org.
[49] A. Andersson, E. Lavonen, M. Harir, M. Gonsior, N. Hertkorn, P. Schmitt-Kopplin, H. Kylin, D. Bastviken, Selective removal of natural organic matter during drinking water production changes the composition of disinfection by-products, Environ. Sci. (Camb.) 6 (2020) 779–794, https://doi.org/10.1039/c9ew00931k.
[50] A. Andersson, M. Harir, M. Gonsior, N. Hertkorn, P. Schmitt-Kopplin, H. Kylin, S. Karlsson, M.J. Ashiq, E. Lavonen, K. Nilsson, Ä. Pettersson, H. Stavklint, D. Bastviken, Waterworks-specific composition of drinking water disinfection by-products, Environ. Sci. (Camb.) 5 (2019) 861–872, https://doi.org/10.1039/c9ew00034h.
[51] C. Postigo, A. Andersson, M. Harir, D. Bastviken, M. Gonsior, P. Schmitt-Kopplin, P. Gago-Ferrero, L. Ahrens, L. Ahrens, K. Wiberg, Unraveling the chemodiversity of halogenated disinfection by-products formed during drinking water treatment using target and non-target screening tools, J. Hazard. Mater. 401 (2021), https://doi.org/10.1016/j.jhazmat.2020.123681.
[52] E.A. Detenchuk, D.M. Mazur, T.B. Latkin, A.T. Lebedev, Halogen substitution reactions of halobenzenes during water disinfection, Chemosphere 295 (2022), https://doi.org/10.1016/j.chemosphere.2022.133866.
[53] B. Chen, H. Shen, Y. Jin, Q. Wu, J. Liu, X. Wang, X. Zhang, H. Yu, Formation mechanisms of chlorinated disinfection byproducts chlorinated benzoquinones from free aromatic amino acids: in vitro and in silico study, Sci. Total Environ. 966 (2025), https://doi.org/10.1016/j.scitotenv.2025.178685.
[54] P. Canosa, I. Rodríguez, E. Rubí, N. Negreira, R. Cela, Formation of halogenated by-products of parabens in chlorinated water, Anal. Chim. Acta 575 (2006) 106–113, https://doi.org/10.1016/j.aca.2006.05.068.
[55] M. Terasaki, Y. Takemura, M. Makino, Paraben-chlorinated derivatives in river waters, Environ. Chem. Lett. 10 (2012) 401–406, https://doi.org/10.1007/s10311-012-0367-1.
[56] A. Janiga-MacNelly, M. McGraw, M.T. Fernandez-Luna, R. Lavado, Assessment of the toxic effects of parabens, commonly used preservatives in cosmetics, and their halogenated by-products on human skin and endothelial cells, NAM J. 1 (2025) 100011, https://doi.org/10.1016/j.namjnl.2025.100011.
[57] Y. Yoon, M. Cho, Detrimental impacts and QSAR baseline toxicity assessment of Japanese medaka embryos exposed to methylparaben and its halogenated byproducts, Sci. Total Environ. 927 (2024), https://doi.org/10.1016/j.scitotenv.2024.171448.
[58] M.A. de Souza Moura, K.M. de Oliveira, G.C. dos Santos Gonçalves, do Nascimento, O.V. Junior, R. da Silva Gonzalez, A.P. Peron, D.C. de Souza, Enzymatic evaluation of the phytoaccumulative capacity of *Salvinia biloba* under stress conditions caused by methylparaben and chlorinated derivatives, Water Air Soil Pollut. 235 (2024) 676, https://doi.org/10.1007/s11270-024-07475-w.
[59] G.C. dos Santos Gonçalves Nascimento, E. Dusman, R. da Silva Gonzalez, J. V. Nicola, M.A. de Souza Moura, K.M. de Oliveira, A.K.G. Oliveira, P.A. Bressani, D. E. Santo, Á.C.K. Filipi, E.M.V. Gomes, J.C. Pokrywiecki, D.C. de Souza, A.P. Peron, Toxicity of methylparaben and its chlorinated derivatives to *Allium cepa L.* and *Eisenia fetida Sav*, Environ. Sci. Pollut. Res. 30 (2023) 57850–57861, https://doi.org/10.1007/s11356-023-26539-8.
[60] S. Zhang, Y. Wang, J. Lu, Z. Yu, H. Song, P.L. Bond, J. Guo, Chlorine disinfection facilitates natural transformation through ROS-mediated oxidative stress, ISME J. 15 (2021) 2969–2985, https://doi.org/10.1038/s41396-021-00980-4.
[61] W.S. da Cruz Nizer, M.E. Adams, K.N. Allison, M.C. Montgomery, H. Mosher, E. Cassol, J. Overhage, Oxidative stress responses in biofilms, Biofilm 7 (2024), https://doi.org/10.1016/j.bioflm.2024.100203.
[62] J.Y. Maillard, I. Centeleghe, How biofilm changes our understanding of cleaning and disinfection, Antimicrob. Resist. Infect. Control 12 (2023), https://doi.org/10.1186/s13756-023-01290-4.
[63] Y. Liu, C. Wang, G. Tyrrell, X.F. Li, Production of Shiga-like toxins in viable but nonculturable *Escherichia coli* O157:H7, Water Res. 44 (2010) 711–718, https://doi.org/10.1016/j.watres.2009.10.005.
[64] S. Zheng, T. Lin, H. Chen, X. Zhang, F. Jiang, Impact of changes in biofilm composition response following chlorine and chloramine disinfection on

nitrogenous disinfection byproduct formation and toxicity risk in drinking water distribution systems, Water Res. 253 (2024), https://doi.org/10.1016/j.watres.2024.121331.
[65] H.Y. Liu, E.L. Prentice, M.A. Webber, Mechanisms of antimicrobial resistance in biofilms, Npj Antimicrob. Resist. 2 (2024) 27, https://doi.org/10.1038/s44259-024-00046-3.
[66] X. Zhang, T. Lin, F. Jiang, X. Zhang, S. Wang, S. Zhang, Impact of pipe material and chlorination on the biofilm structure and microbial communities, Chemosphere 289 (2022), https://doi.org/10.1016/j.chemosphere.2021.133218.
[67] K. Miksch, B. Kończak, Distribution of extracellular polymeric substances and their role in aerobic granule formation, Chem. Process. Eng. 33 (2012) 679–688, https://doi.org/10.2478/v10176-012-0057-3.
[68] Vandana, M. Priyadarshanee, S. Das, Bacterial extracellular polymeric substances: biosynthesis and interaction with environmental pollutants, Chemosphere 332 (2023), https://doi.org/10.1016/j.chemosphere.2023.138876.
[69] L.C.A. de Araújo, A.F. da Purificação-Júnior, S.M. da Silva, A.C.S. Lopes, D. L. Veras, L.C. Alves, F.B. dos Santos, T.H. Napoleão, M.T. dos Santos Correia, M. V. da Silva, M.L.V. Oliva, M.B.M. de Oliveira, In vitro evaluation of mercury (Hg2 +) effects on biofilm formation by clinical and environmental isolates of *Klebsiella pneumoniae*, Ecotoxicol. Environ. Saf. 169 (2019) 669–677, https://doi.org/10.1016/j.ecoenv.2018.11.036.
[70] V. Arruda, M. Simões, I. Gomes, The impact of synthetic musk compounds in biofilms from drinking water bacteria, J. Hazard. Mater. (2022) 129185, https://doi.org/10.1016/j.jhazmat.2022.129185.
[71] H. Wang, C. Hu, Y. Shen, B. Shi, D. Zhao, X. Xing, Response of microorganisms in biofilm to sulfadiazine and ciprofloxacin in drinking water distribution systems, Chemosphere 218 (2019) 197–204, https://doi.org/10.1016/j.chemosphere.2018.11.106.
[72] L. Cao, Y. Liao, C. Su, L. Tang, Z. Qi, L. Wei, J. Wu, S. Gao, Effects of PFOA on the physicochemical properties of anaerobic granular sludge: performance evaluation, microbial community and metagenomic analysis, J. Environ. Manag. 313 (2022), https://doi.org/10.1016/j.jenvman.2022.114936.
[73] Y. Zhang, Z. Qv, J. Wang, Y. Yang, X. Chen, J. Wang, Y. Zhang, L. Zhu, Natural biofilm as a potential integrative sample for evaluating the contamination and impacts of PFAS on aquatic ecosystems, Water Res. 215 (2022), https://doi.org/10.1016/j.watres.2022.118233.
[74] H.-C. Flemming, E.D. van Hullebusch, T.R. Neu, P.H. Nielsen, T. Seviour, P. Stoodley, J. Wingender, S. Wuertz, The biofilm matrix: multitasking in a shared space, Nat. Rev. Microbiol. 21 (2023) 70–86, https://doi.org/10.1038/s41579-022-00791-0.
[75] C. Gao, M. Habibi, T.L.G. Hendrickx, H.H.M. Rijnaarts, H. Temmink, D. Sudmalis, Variation of viscoelastic properties of extracellular polymeric substances and their relation to anaerobic granule's mechanical strength in full-scale treatment plants, Bioresour. Technol. 411 (2024), https://doi.org/10.1016/j.biortech.2024.131233.
[76] Z. Wang, J. Kim, Y. Seo, Influence of bacterial extracellular polymeric substances on the formation of carbonaceous and nitrogenous disinfection byproducts, Environ. Sci. Technol. 46 (2012) 11361–11369, https://doi.org/10.1021/es301905n.
[77] Z. Xue, Y. Seo, Impact of chlorine disinfection on redistribution of cell clusters from biofilms, Environ. Sci. Technol. 47 (2013) 1365–1372, https://doi.org/10.1021/es304113e.
[78] Z. Dai, M.C. Sevillano-Rivera, S.T. Calus, Q.M. Bautista-De Los Santos, A.M. Eren, P.W.J.J. Van Der Wielen, U.Z. Ijaz, A.J. Pinto, Disinfection exhibits systematic impacts on the drinking water microbiome, Microbiome 8 (2020), https://doi.org/10.1186/s40168-020-00813-0.
[79] X. Ruotong, X. Jiayi, C. Ruisi, T. Yulin, Z. Yongji, Effect of antibiotics and antibiotic by-products on the chlorine resistance of biofilms in drinking water distribution systems, J. Water Process Eng. 66 (2024), https://doi.org/10.1016/j.jwpe.2024.105987.
[80] I.C. Pinto, M. Simões, I.B. Gomes, The effects of emerging contaminants on the behaviour of *Acinetobacter calcoaceticus* derived from biofilms, Environ. Sci. (Camb.) 9 (2023) 74–85, https://doi.org/10.1039/D2EW00246A.
[81] J. Subirats, X. Timoner, A. Sànchez-Melsió, J.L. Balcázar, V. Acuña, S. Sabater, C. M. Borrego, Emerging contaminants and nutrients synergistically affect the spread of class 1 integron-integrase (*intI1*) and *sul1* genes within stable streambed bacterial communities, Water Res. 138 (2018) 77–85, https://doi.org/10.1016/j.watres.2018.03.025.
[82] Y. Wang, J. Lu, L. Mao, J. Li, Z. Yuan, P.L. Bond, J. Guo, Antiepileptic drug carbamazepine promotes horizontal transfer of plasmid-borne multi-antibiotic resistance genes within and across bacterial genera, ISME J. 13 (2019) 509–522, https://doi.org/10.1038/s41396-018-0275-x.
[83] E.M. Hartmann, R. Hickey, T. Hsu, C.M. Betancourt Román, J. Chen, R. Schwager, J. Kline, G.Z. Brown, R.U. Halden, C. Huttenhower, J.L. Green, Antimicrobial chemicals are associated with elevated antibiotic resistance genes in the indoor dust microbiome, Environ. Sci. Technol. 50 (2016) 9807–9815, https://doi.org/10.1021/acs.est.6b00262.
[84] S. Rabow, M. Soares, J. Rousk, Can heavy metal pollution induce soil bacterial community resistance to antibiotics in boreal forests? J. Appl. Ecol. 60 (2023) 237–250, https://doi.org/10.1111/1365-2664.14322.
[85] I. González-Mariño, J.B. Quintana, I. Rodríguez, R. Cela, Evaluation of the occurrence and biodegradation of parabens and halogenated by-products in wastewater by accurate-mass liquid chromatography-quadrupole-time-of-flight-mass spectrometry (LC-QTOF-MS), Water Res. 45 (2011) 6770–6780, https://doi.org/10.1016/j.watres.2011.10.027.